

---

**ADDIS ABABA UNIVERISTY**  
**DEPARTMENT OF CHEMIISTRY**



**ELECTROCHEMICAL CHARACTERIZATION AND  
DETERMINATION OF CATECHOL AT POLY BCP/ERGO/GC  
MODIFIED ELECTRODE**

**BY**  
**MEDHIN BAHTA NIGUSSIE**

**ADVISOR**  
**NEGUSSIE NEGASH (PhD)**

**April, 2018**

---

**ELECTROCHEMICAL CHARACTERIZATION AND  
DETERMINATION OF CATECHOL AT POLY BCP/ERGO/GC  
MODIFIED ELECTRODE**

**BY  
MEDHIN BAHTA NIGUSSIE**

**A GRADUATE THESIS SUBMITTED TO THE DEPARTMENT OF  
CHEMISTRY IN PARTIAL FULFILMENT OF THE  
REQUIRMENTS FOR THE DEGREE OF MASTER OF  
SCIENCE IN CHEMISTRY**

**Addis Ababa University  
Addis Ababa, Ethiopia**

**April, 2018**

---

**ADDIS ABABA UNIVERISTY**  
**DEPARTMENT OF CHEMIISTRY**

**ELECTROCHEMICAL CHARACTERIZATION AND DETERMINATION  
OF CATECHOL AT POLY BCP/ERGO/GC MODIFIED ELECTRODE**

**BY**  
**MEDHIN BAHTA NIGUSSIE**

Approved by the examining board

Signature

Negussie Negash (PhD) (Advisor)

\_\_\_\_\_

Merid Tessema (PhD) (Examiner)

\_\_\_\_\_

Weldegebriel Yohannes (PhD) (Examiner)

\_\_\_\_\_

April, 2018

---

## Acknowledgements

First, I have to thank God for giving me the gift that He did and for everyday for everything that happens to me.

I would like to express my deep and sincere gratitude to my advisor Negussie Negash (PhD). I am grateful for all his guidance, motivation, and friendly approach during this work.

I sincerely thank Tesfu Hailu (Analytical chemistry PhD student), for his sincere guidance, technical aid and assistance in every day laboratory problems facing me in the research direction.

I would like to thank Addis Ababa University, Department of Chemistry for providing me with the necessary knowledge, all assistances, facilities, soft copies and material support to conduct the thesis work.

I would like to show my warm thank to the head of the Department of chemistry, Ahmed Mustefa (PhD), Merid Tessema (PhD), Estifanos Elile (PhD), and Mesfin Redi (PhD) whose reminders and constant motivation encouraged me to meet the deadline.

I would like to extend special gratitude and appreciation to Brehane Kahsay, Hailemical Kahsay and his wife Selam, Gebremeskel Kahsay (PhD) and my sister Abeba for their support morally and emotionally.

I am grateful to my friends Beshatu Gerba, Binyam Berihu, and Sentayehu Abebe and all my class mates for their support and making my time enjoyable at Addis Ababa University.

Lastly but not least my heartfelt gratitude shall go to my family, my husband Leakemariam Berehe (PhD) and my daughters Simret and Selam for providing me unfailing support during this program.

---

# Table of Contents

ACKNOWLEDGEMENTS .....	I
LIST OF FIGURES.....	IV
LIST OF TABLES .....	VII
ABSTRACT .....	X
1. INTRODUCTION.....	1
1.1 OBJECTIVE.....	3
1.1.1 General Objective.....	3
1.1.2 SPECIFIC OBJECTIVES.....	3
2. REVIEW OF LITERATURE.....	3
2.1 CATECHOL (CC).....	3
2.1.1 Physical Properties of Catechol.....	3
2.1.2 Production and Use .....	4
2.1.3 Occupational Exposure.....	4
2.1.4 Environmental Occurrence.....	4
2.1.5 Molecular Modes of Action of Catechols in Cells.....	5
2.1.6 Determination of Catechol .....	7
2.2 ELECTROCHEMICAL SENSORS.....	9
2.2.1 Chemically Modified Electrodes.....	10
2.2.2 Purpose of Developing Chemically Modified Electrodes.....	10
2.2.3 Applications of Chemically Modified Electrodes.....	11
2.2.4 Allotropes of Carbon .....	11
2.2.5 Carbon Nanotubes (CNTs).....	12
2.3 GRAPHENE AND SENSORS.....	12
2.3.1 Structure of Graphene .....	12
2.3.2 Preparation of Graphene.....	13
2.4 GRAPHENE OXIDE (GO).....	14
2.4.1 Preparation of Graphene Oxide.....	14
2.4.2 Synthesis of Electrochemically reduced Graphene oxide (ERGO).....	16
2.4.5 Advantages of ERGO Compared to CRGO .....	20
2.5 CONDUCTING POLYMERS (CPS) .....	21
2.6 BROMOCRESOL PURPLE.....	24
2.7 THE ELECTROCHEMICAL CELL .....	26
2.7.1 The Working Electrode .....	26
2.7.2 The Function of the Working Electrode.....	26
2.7.3 Selection of Working Electrode .....	27
2.7.4 Types of Working Electrodes.....	27

---

2.7.5	Glassy Carbon Electrode .....	27
2.7.6	Modified Electrodes .....	28
2.8	GENERAL THEORY OF CYCLIC AND DIFFERENTIAL PULSE VOLTAMMETRY .....	29
2.8.1	Voltammetric Sensing Principles .....	29
2.8.2	Electrochemical Reversibility and Irreversibility.....	30
2.8.3	Cyclic voltammetry .....	33
2.8.4	Differential Pulse Voltammetry .....	36
2.8.5	The supporting electrolyte.....	37
2.8.6	The Potentiostat.....	37
3	EXPERIMENTAL .....	38
3.1	REAGENTS AND CHEMICALS.....	38
3.2	APPARATUS AND INSTRUMENTATION.....	38
3.2.1	Apparatus.....	38
3.2.2	Instrumentation.....	39
3.3	EXPERIMENTAL PROCEDURE .....	39
3.3.1	Preparation of Supporting Electrolytes .....	39
3.3.2	Preparation of Analyte and Modifier Solutions .....	40
3.3.3	Preparation of Interference Solutions.....	40
3.4	ELECTRODE MODIFICATION .....	40
3.4.1	Preparation of the Glassy Carbon Electrode for Modification.....	40
3.4.2	Modification of the glassy carbon electrode with ERGO .....	40
3.4.3	Modification of ERGO/GC Electrode with poly BCP .....	41
4	RESULTS AND DISCUSSION .....	42
4.1	COMPARISON OF BARE, POLY BCP/GCE, ERGO/GCE AND POLY BCP/ERGO/GCE.....	42
4.2	ELECTROCHEMICAL RESPONSES FOR CC AT POLY BCP/ERGO/GCE .....	43
4.3	CYCLIC VOLTAMMETRIC ANALYSES OF CATECHOL.....	45
4.3.1	Effect of scan rate.....	47
4.3.2	Effect of pH of the supporting electrolyte.....	49
4.4	DIFFERENTIAL PULSE VOLTAMMETRIC ANALYSIS.....	50
4.4.1	Optimization of DPV Experimental Parameters .....	50
4.4.2	Linear Range and Detection Limit .....	51
4.4.3	Comparison with Reported works .....	53
4.4.4	Effect of Interferences .....	53
4.4.5	Determination of CC in Tap water .....	57
5	CONCLUSIONS.....	59
6	REFERENCES.....	60

---

## List of Figures

Figure 1: a) Structural formula b) 3D Structural formula of CC.....	3
Figure 2: Oxidation mechanism of catechol (CC) .....	5
Figure 3: DNA damages: (A) Formation of 8-hydroxy-20-deoxyguanisine (8-oxo-dG) by the ..... reaction of guanine with hydroxyl radicals. (B) DNA adducts formation by the reaction of catechol estrogens with guanidines .....	6
Figure 4: Three possible forms of catechol ± protein interactions. A) Reaction of oxidized catechol with sulphhydryl groups. B) Reaction of oxidized catechol with amino groups, for example the 1- amino group of lysine C) Reduction of the semiquinone radical by a sulphhydryl group and subsequent protein cross-linking in the presence of oxygen. ....	7
Figure 5: Reaction of Catechol at the modified electrode surface. ....	9
Figure 6: The allotropes of Carbon .....	11
Figure 7: Schematic presentations of Carbon nano tubes .....	12
Figure 8: Structure of graphene: A) Schematic view of the $sp^2$ hybridization. The orbital's form angles of $120^\circ$ . B) Benzene molecule ( $C_6H_6$ ). C) Graphene where $\pi$ electrons are delocalized over the whole structure. ....	13
Figure 9: Schematic illustration of Oxidation of graphite .....	14
Figure 10: Chemical structural model of graphene oxide .....	14
Figure 11: Chemical structure model of the graphite oxide and graphene oxide .....	16
Figure 12: Chemical structure of graphene oxide, and reduced graphene oxide (RGO) .....	17
Figure 13: The electrochemical reduction of GO films coated on; a) insulating substrate and b) conductive substrate to ERGO film .....	18
Figure 14: Schematic illustration of electrochemical reduction approach for production of ERGO .....	20
Figure 15: a) Molecular structure of bromocresol purple. b) 3D structure .....	25
Figure 16 Reversible redox reaction of BCP.....	25
Figure 17: Image of glassy carbon electrodes .....	28

---

Figure 18: The rate of charge transfer $v_{ct}$ , and the rate of mass transport $v_{mt}$ of an electrode reaction .....	31
Figure 19: The relation of the rate of charge transfer $v_{ct}$ to the rate of mass transport $v_{mt}$ for a reversible electrochemical system.....	32
Figure 20: Potential –time excitation signal in cyclic voltammetric experiment.....	33
Figure 21: A cyclic voltammogram .....	34
Figure 22: Differential Pulse Voltammetry a) an anodic scanning of the potential vs time; b) Plot of voltammogram .....	36
Figure 23: The circuit for potentiostat .....	38
Figure 24: The electrochemical cell for voltammetric determination.....	39
Figure 25: Cyclic voltammogram of the electrochemical reduction of GO film on glassy carbon electrode in phosphate buffer solution at a pH 6 in the potential range -1.2 V to 2.0 V vs Ag/AgCl/(3 M KCl) at scan rate of 100 mV/s for 15 cycles.....	41
Figure 26: Cyclic voltammogram for the electropolymerization of $5 \times 10^{-2}$ M bromocresol purple monomer in a 0.1 M phosphate buffer (pH-6) in the potential range of -0.10 V-1.60 V versus Ag/AgCl (3 M KCl) at a scan rate of 100 mV/s for 15 cycles on electrochemical reduced GO modified electrode (ERGO/GCE).....	42
Figure 27: Cyclic voltammogram of 100 $\mu$ M catechol at different electrodes (a) bare GCE (b)poly BCP/GCE c) ERGO)/GCE, and d) poly BCP/ERG/GCE at scan rate of 100 mVs <sup>-1</sup> in 0.1 M ABS solution pH 6.0. ....	43
Figure 28: Cyclic voltammetric signals of $5 \times 10^{-2}$ M $[\text{Fe}(\text{CN})_6]^{3-}/[\text{Fe}(\text{CN})_6]^{4-}$ in 0.1 M KCl (equimolar) at a scan rate of 100 mV/s: a) Bare GCE b) poly BCP/ERGO/GCE .....	45
Figure 29: Cyclic voltammogram of 0.1 mM CC in pH of 6 ABS and scan rate of 100 mV/s .....	46
Figure 30 Electrochemical oxidation reaction of CC at the poly BCP/ERGO/GC modified electrode .....	46
Figure 31: Cyclic voltammogram recorded at poly BCP/ERGO/GCE for $10^{-4}$ M CC in 0.1 M acetate buffer solution (pH 6.0) at different scan rates (mV/s) 25, 50, 100, 150, 200, 250, 300, 350, 400, 450, 500, 550, and 600. ....	<b>Error! Bookmark not defined.</b>
Figure 32: The dependence of the anodic and cathodic peak currents on square root of scan rate	48
Figure 33: The dependence of the anodic and cathodic peak potential ( $E_p$ ) on log of scan rate mVs <sup>-1</sup> .....	<b>Error! Bookmark not defined.</b>

---

Figure 34: The effects of pH on the response for $10^{-4}$ M catechol in 0.1 M acetate buffer solution at poly BCP/ ERGO/GCE at scan rate of $100 \text{ mVs}^{-1}$ a) pH 5 b) pH 6 c) pH 7 d) pH 7.5 e) pH 8...	49
Figure 35 Plot of anodic peak currents as a function of pH for $10^{-4}$ M catechol at $100 \text{ mVs}^{-1}$ .....	50
Figure 36: Differential pulse voltammograms at poly BCP/ERGO/GC modified electrode for different concentrations of catechol .....	52
Figure 37: Plot of DPV anodic peak current as a function of catechol concentration from 5-30 $\mu\text{M}$ .....	53
Figure 38 Differential pulse voltammograms at poly BCP/ERGO/GC modified electrode for 20 $\mu\text{M}$ CC and a) 20 b) 60 and c) 100 $\mu\text{M}$ ascorbic acid (AA) .....	54
Figure 39 Differential pulse voltammograms at poly BCP/ERGO)/GC modified electrode in a 0.1 M ABS (pH-6) for a) 20 b) 100 and c) 200 $\mu\text{M}$ hydroquinone (HC) spiked to 20 $\mu\text{M}$ CC...	55
Figure 40 Differential pulse voltammograms at poly BCP/ERGO/GC modified electrode in a 0.1 ABS (pH-6) for a) 20 b) 60 c) 100 and d) 200 $\mu\text{M}$ phenol spiked to 20 $\mu\text{M}$ CC.....	56
Figure 41 Possible redox reactions of phenol at the electrode .....	56
Figure 42 Differential pulse voltammogram at poly BCP/ERGO/GC modified electrode in a 0.1 ABS (pH-6) for a) 20 b) 40 and c) 60 $\mu\text{M}$ dichlorophenol spiked to 20 $\mu\text{M}$ CC.....	57
Figure 43 Differential pulse voltammograms at poly BCP/ERGO/GC modified electrode in 0.1 M ABS (pH-6) for a) 500 b)1000 c)1500 d) 2000 and e) 2500 $\mu\text{L}$ of $10^{-4}$ M spiked to 6 mL ABS and 4 mL of tap water.....	58

---

## List of Tables

Table 1 Molecular structures of some conjugated polymers and their repeating unit .	21
Table 2 Structures and doping chemicals of some common conducting polymers	23
Table 3 Electrical Conductivity of Some Conjugated Polymers	24
Table 4 Electrochemical Response Measurement at poly BCP/ERGO/GCE	44
Table 5 Parameters and Optimum Values of DPV Experimental Conditions	51
Table 6: Comparison of Characteristics Values Obtained from Some Literatures and This Work.	53
Table 7 Recovery Study	58

---

## List of Abbreviations

CC	Catechol
BCP	Bromocresol purple
Poly BCP	polymer of bromocresol purple
GO	Graphene oxide
ERGO	Electrochemically reduced graphene oxide
CRGO	Chemically Reduced Graphene oxide
MWCNTs	Multi Wall Carbon Nanotubes
SWCNT	Single Wall Carbon Nano Tube
WE	working electrode
RE	Reference electrode
CE	Counter electrode
GCE	Glassy carbon electrode
CNTs	Carbon nanotubes
CME	Chemically modified electrode
CPs	Conducting polymers
ICPs	Intrinsically conducting polymers
CV	Cyclic voltammetry
LSV	Linear Sweep Voltammetry
$v_{mt}$	Rate of mass transfer
$v_{ct}$	Rate of charge transfer
DPV	Differential pulse voltammetry
E	Potential
$\Delta E$	Change in potential
$E_{1/2}$	Half wave potential
$E_{pc}$	Cathodic peak potential
$E_{pa}$	Anodic peak potential
HQ	Hydroquinone
I	Current
A	Ampere

---

$\mu\text{A}$	Microampere
$i_{\text{pa}}$	Anodic peak current
$i_{\text{pc}}$	Cathodic peak current
M	Molar
mM	milli molar
$\mu\text{M}$	Micro molar
$\mu\text{L}$	Micro liter
n	Number of electron
PBS	Phosphate buffer solution
ABS	acetate buffer solution
s	Second
AA	Ascorbic acid
D	Diffusion coefficient
R	Regression Coefficient
GC	Gas Chromatography
HPLC	High Performance Liquid Chromatography
MC	Mass Spectroscopy
DNA	Deoxyribonucleic Acid
PEDOT	Poly 3, 4-Ethylene dioxythiophene

---

## Abstract

A glassy carbon electrode was modified with a poly bromocresol purple and electrochemically reduced graphene oxide. The modified electrode was characterized, and used to electrochemically determine catechol (1, 2-dihydroxy benzene, CC) using cyclic and differential pulse voltammetry and exhibited good electrocatalytic activities toward the oxidation of CC. The peak currents were linear with the CC concentrations in the range of 5–140  $\mu\text{M}$  with a 0.998 correlation coefficient and a corresponding detection limits of 0.8  $\mu\text{M}$  . The effect of hydroquinone, ascorbic acid, phenol and dichlorophenol as interfering substances on the peak current of catechol was examined using differential pulse voltammetry. The modified electrode exhibited good sensitivity, and reproducibility for the determination of CC indicating the promising applications of the modified electrode in real sample analysis.

Keywords: Electroanalytical; Catechol; conducting polymers; electropolymerization; bromocresol purple; electrochemically reduced graphene oxide; modified electrode; and voltammetry.

---

## 1. Introduction

The definition of analytical chemistry was given by the Federation of European Chemical Societies (FECS) and adopted by IUPAC: “develops and applies methods, instruments and strategies to obtain information on the composition and nature of matter in space and time, as well as on the value of these measurements, that is their uncertainty, validation, and/or traceability to fundamental standards.” [1]

Electroanalytical chemistry, also known as electroanalysis, lies at the interface between analytical science and electrochemistry. The history of electrochemical sensors starts basically with the development of glass electrode by Cremer in 1906. Haber and his student Klemensiewicz took up the idea in 1909 and made the basis for analytical application. Today, the electrochemical sensor plays an essential analytical role in the fields of environmental conservations and monitoring, disaster, disease prevention, and industrial analysis [1].

Electrocatalytic processes in Electroanalytical chemistry play crucial role in a number of contemporary technologies, facing the scientific and engineering community with the necessity of having powerful and versatile techniques for the investigation of these processes. In this sense, voltammetric techniques present irreplaceable tools due to their fastness and ability to provide a vast amount of important thermodynamics and kinetics information [1].

Catechol (1,2-dihydroxy benzene or CC) is present in wide range of natural compounds and produced in most of the industrial processes. It is found mainly in biological, particularly in neurological compounds. In addition to that, it has wide range of applications such as, precursor to flavors, fragrances, in the field of agriculture (pesticides, insecticide) medicines (pharmaceuticals), and photographic chemicals. Beside these applications, its concentration in various body fluids gives the information about the neural diseases such as neuroblastoma, its increased concentration levels toxic to the aquatic, plants, animals and human life; make the detection of CC significant [2].

It is of great significance to develop a fast reliable and inexpensive analytical method for determination of trace amounts of chemical residue. The identification and quantification of chemical residues are generally based on chromatographic methods such as gas chromatography (GC) and high-performance liquid chromatography (HPLC) coupled with mass spectroscopy (MS).

---

These methods are very sensitive and reliable; however they are time consuming and expensive. Moreover, they require a qualified and experienced staff, and are not convenient for in-vivo, in-vitro, in situ or on site detection [3].

Various analytical methods have been developed for the detection of CC, such as capillary electrophoresis, liquid-phase chromatography, electrochemical and flow injection analyses which were most commonly used techniques. Among these, electrochemical method has great importance due to its simple, cost effective and fast response. Carbon electrodes such as graphite, glassy carbon and its modification such as, graphene oxide, electrochemical pretreatment and Carbon nanotubes have shown better results as sensor materials [3]

The use of new materials, especially nanomaterials, has become an increased area of research in electrochemical sensors. The incorporation of these nanomaterials in conjugation with one another to form novel composites is becoming very important, as many of these materials have been found synergistic effects. Amperometric sensors based on glassy carbon modified with electrochemically reduced graphene oxide and polymer composite film are one of the recent advances in the electrochemical sensors [4].

Although the useful surface layers can be designed for particular reactions of interest (here CC), practical catalysts that satisfy all analytical and physical properties have not yet emerged; this remains an important and promising area of research. An electrochemical sensor modified by poly-bromocresol purple composite over electrochemically reduced graphene oxide on glassy carbon electrode, symbolized as poly BCP/ERGO/GC modified electrode was used for electrochemical characterization and determination of catechol at this electrode. The electrochemical behavior of catechol (CC) at this modified electrode was studied by cyclic and differential pulse voltammetry.

---

## 1.1 Objective

### 1.1.1 General Objective

To synthesize and characterize poly bromocresol purple and electrochemically reduced graphene oxide film composite on glassy carbon electrode and use as a sensor for the voltammetric determination of catechol.

### 1.1.2 Specific Objectives

To characterize the electrocatalytic activity of poly bromocresol purple electrochemically reduced graphene oxide film composite on glassy carbon electrode.

To optimize the basic electroanalytical parameters required for the sensitive determination of catechol at the poly BCP/ERGO/GC modified electrode using CV and DPV.

## 2. Review of Literature

### 2.1 Catechol (CC)

Phenols with two hydroxyl groups, such as catechol, are called Benzenediols. Catechol has a chemical formula of  $C_6H_4(OH)_2$  with relative molecular mass of 110.11g/mol and its structure formula is shown in Figure 1.

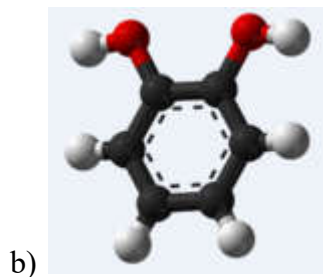
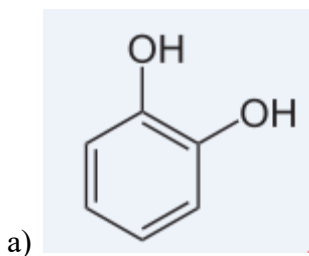


Figure 1: a) Structural formula b) 3D Structural formula of CC

#### 2.1.1 Physical Properties of Catechol

Catechol in pure state is colorless monoclinic crystals. It has a boiling-point of 245°C and a melting-point of 105°C. It is very soluble in water, benzene, chloroform, diethyl ether, ethanol, pyridine and aqueous alkalis. It has a Vapor pressure of 4 Pa at 20°C, and relative vapor density (air = 1), 3.79. It's flash-point is 127.2°C, open cup [5].

---

### **2.1.2 Production and Use**

Worldwide consumption of catechol in 1980 was estimated to be about 20 thousand tones. Catechol is currently produced in France, Italy, Japan, the United Kingdom and the United States. Approximately 50% is used as starting material for insecticides, 35–40% for perfumes and drugs and 10–15% for polymerization inhibitors and other chemicals. Catechol has also been used as an antiseptic, in photography, dyestuffs, electroplating, specialty inks, antioxidants, light stabilizers, and in organic synthesis [5].

### **2.1.3 Occupational Exposure**

According to the 1981–83 National Occupational Exposure Survey (NOES, 1997), approximately 14000 workers in the United States were potentially exposed to catechol. Occupational exposures to catechol may occur in its production, in the production of insecticides, perfumes drugs, in metal-plating shops and in coal processing. Skin contact with catechol cause eczema tics in humans. In humans, absorption through the skin results in an illness resembling that induced by phenol, except convulsions are more pronounced. Large doses of catechol can cause depression of the central nervous system (CNS) and a prolonged rise of blood pressure in animals. Tumors in glandular stomach were observed in orally exposed rats. The International Agency for Research on cancer (IARC) has classified catechol as group 2B, possible human carcinogen [5].

### **2.1.4 Environmental Occurrence**

Catechol occurs naturally in fruits and vegetables such as onion, apple and crude beet sugar, and in trees such as pine, oak and willow. Catechol may be released to the environment during its manufacture and use. It has been detected at low levels in ambient and urban air, groundwater, drinking-water and soil samples. It has been also found in waste waters from coal conversion, coal-tar chemical production and bituminous shale. It is present in cigarette smoke at 100–360 µg per cigarette [5]. Catechol is one of the common building blocks in organic synthesis and is produced in industrial scales as the precursor of pesticides, perfumes, and pharmaceuticals. The catechol skeleton also occurs in variety of natural products specially the antioxidant. The most well-known characteristic of the catechols is that they can be easily oxidized mainly due to their antioxidant activity and low oxidation potentials [5].

## 2.1.5 Molecular Modes of Action of Catechols in Cells

Catechols can act both as antioxidant, preventing lipid peroxidation, and as pro-oxidant damaging macromolecules such as DNA and proteins. Catechols can also destroy membrane functioning due to their redox cycling activity [6]:

1. Redox Cycling: as seen in the Figure 2 below in the redox cycling reaction it produces the reactive intermediate species.

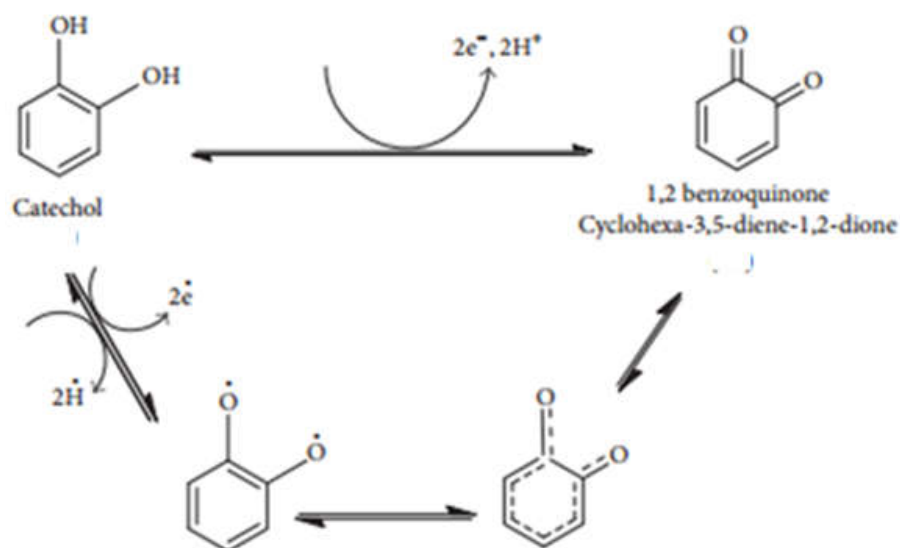
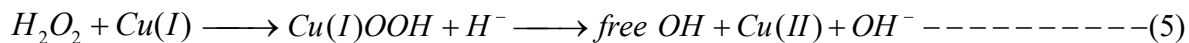
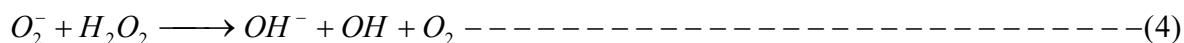
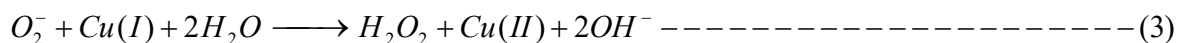
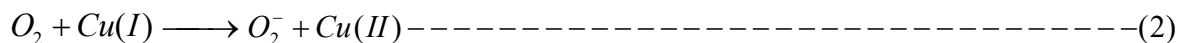


Figure 2: Oxidation mechanism of catechol (CC) [6].

Some of the molecular modes of actions of CC are given below. Catechol as such does not cause oxidative DNA damage in vitro, but the reactive intermediate species of CC combined with heavy metals (e.g.  $\text{Cu}^{2+}$ ,  $\text{Fe}^{3+}$ ), and produce reactive oxygen species (ROS). The following reactions of Catechol with heavy metals and oxygen are some of the examples [7]:



## 2. DNA damage (for example, strand breaks and DNA adduct formation)

Simple phenol structures like catechol react differently when in the cell. Catechol is a relatively non-polar molecule which allows it to be easily taken up by the cells but not easily expelled. The unbalanced accumulation of any foreign species in the cells can lead to the destruction of the cell. Furthermore, upon oxidation, catechol acts very similar to the previously mentioned free radicals and will bind to critical cell components such as lipids, proteins and DNA. The binding destroys the functionality of the component in the cell as illustrated in figure 3. Catechol was deemed a hazardous pollutant and studies have shown that it may even have carcinogenic effects on cells [7].

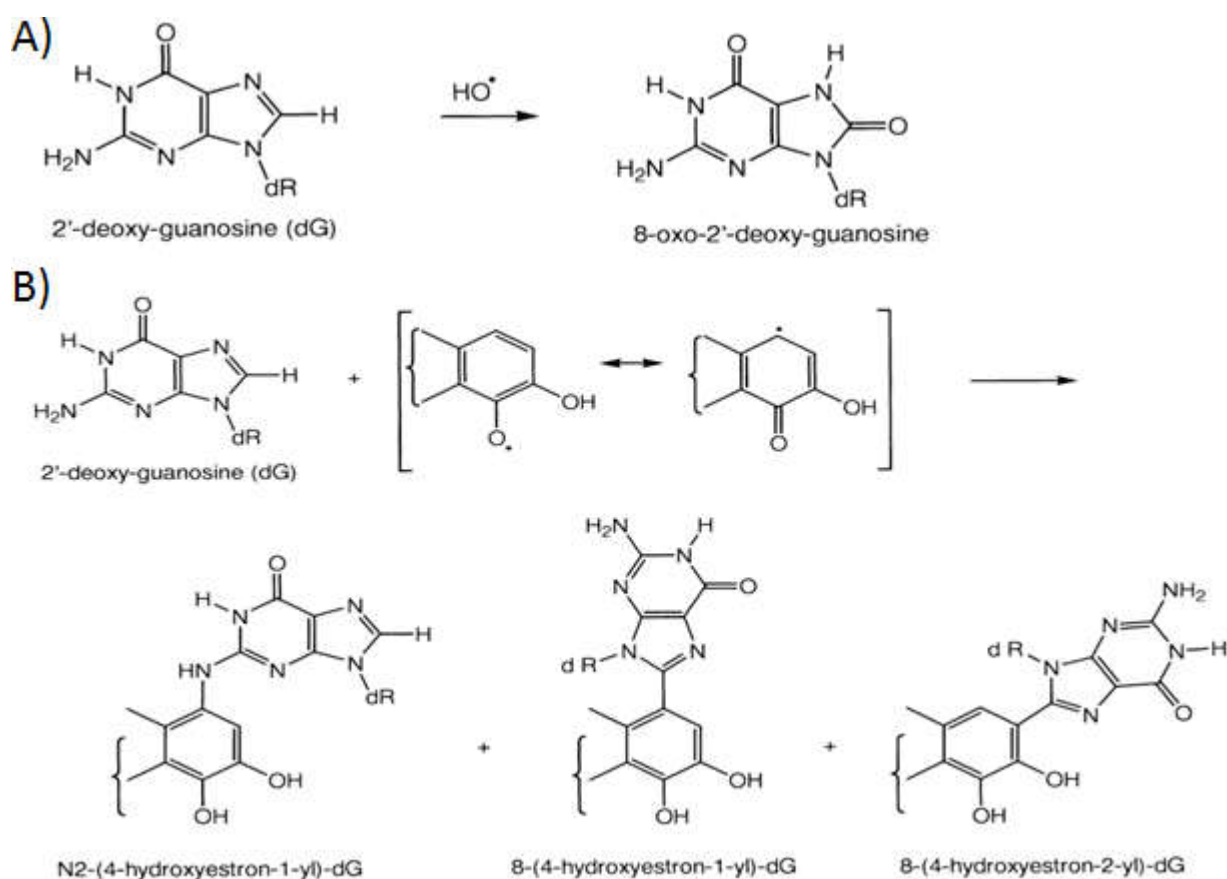


Figure 3: DNA damages: (A) Formation of 8-hydroxy-20-deoxyguanisine (8-oxo-dG) by the reaction of guanisine with hydroxyl radicals. (B) DNA adducts formation by the reaction of catechol estrogens with guanidines [7].

3. Protein damage (for example, protein cross-linking via disulphide groups), and absorption in membranes are possible interactions. Three possible forms of catechol ± protein interactions are given in figure 4 below.

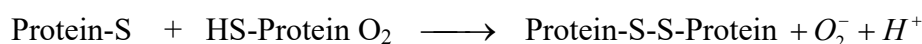
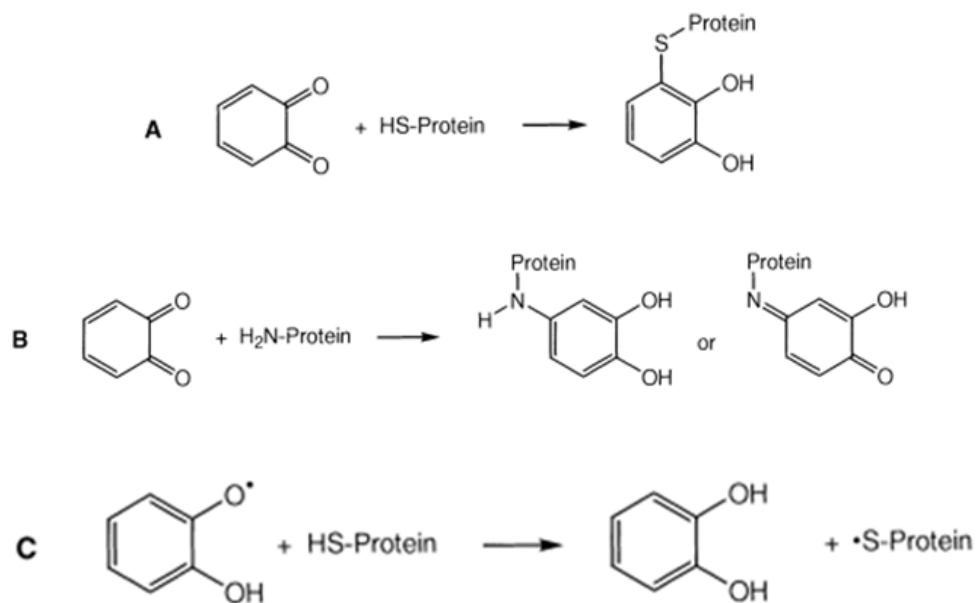


Figure 4: Three possible forms of catechol ± protein interactions. A) Reaction of oxidized catechol with sulphhydryl groups. B) Reaction of oxidized catechol with amino groups, for example the 1-amino group of lysine C) Reduction of the semiquinone radical by a sulphhydryl group and subsequent protein cross-linking in the presence of oxygen.

### 2.1.6 Determination of Catechol

Different methods have been devised for detecting the concentration levels of catechol and other similar phenols. The task is difficult because of the existence of numerous different phenols, not all of which are harmful. Providing adequate selectivity for detecting one phenol over another is a challenge for any proposed sensor. The oxidation or reduction process can be either chemically or electrochemically stimulated. Catechol becomes an o-quinone following oxidation and is reverted back to its original form following reduction. The o-quinone is highly unstable and will readily bond to any nucleophilic surface. The toxicity to cells results from these o-quinones binding to vital

---

cell structures, but this readily binding nature can be taken as advantage to detect the concentration of the o-quinones as they bind to a particular surface [8].

The oxidation of phenols like catechol or of many other types of organic molecules can be electrically stimulated at the anode surface during an electrochemical reaction. This controlled reaction can be measured as a current change which results from the oxidation of the target molecules of catechol. The amplitude of the measured current is directly proportional to the concentration of the oxidized analytes in the solution. Thus, it is necessary to catalyze these reactions by introducing suitable, stable, layers to the electrode surface. It is hoped that by applying known chemical principles about structure and reactivity, useful surface layers can be designed for particular reactions of interest. To amplify the resulting signal and achieve selectivity, of oxidizing enzymes as modifier of electrodes for CC determination [8] such as, polyphenol oxidase (PPO) or lactase [8], SWCNT/PEDOT/GCE [9], screen printed graphite electrode [10], 4, 4-bipyridine/GCE [11], L-cysteine and ZnS:Ni/ZnS QDs on the surface of glassy carbon electrode (ZnS:Ni/ZnS at L-Cys/GCE)[12], anthraquinone modified carbon paste electrode [13], Penicillamine/GCE[14], Tyr/GCE [15], CILE/GCE [16] MWCNT/GCE [17] p-Phe/GCE [18] ---etc, were investigated.

The study of modified electrodes remains a field of high activity. Many new types of surface structures are being prepared, and electrochemical studies are leading to better insights into the way charge is transported through surface layers and how charge is exchanged between surface species and molecules in solution. In other words all actual (practical) applications that must be considered when developing and commercializing electrochemical and biological modified electrodes have not yet developed; many promising possibilities lie on the horizon [19]. Poly BCP/ERGO/GC modified electrode is one of this used for the determination of CC which is simple, cheap, fast, selective, reproducible stable, and gives comparable result with the modifiers still developed.

The electrochemically modified electrodes are used to electrochemically oxidize catechol in the vicinity of the working electrode. Catechol from solution diffuses through the polymer matrix and is oxidized/ reduced at the modified electrode surface as illustrated in figure 5.

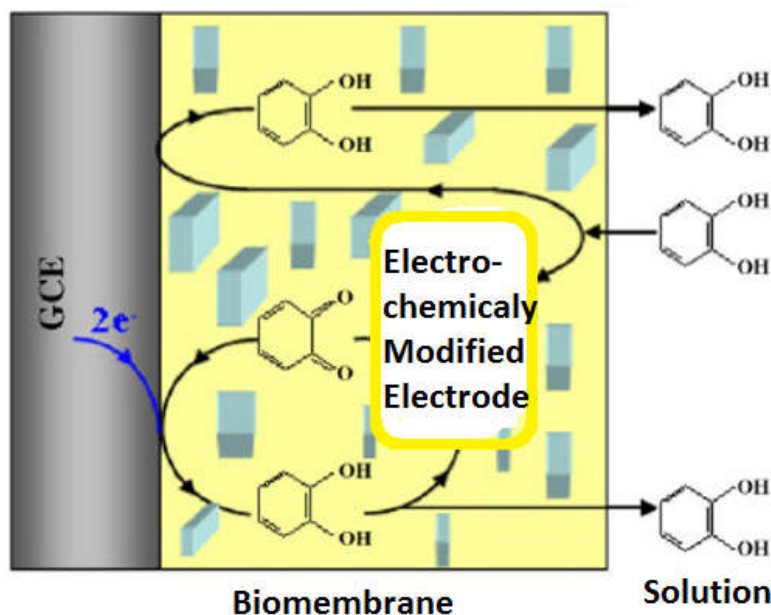


Figure 5: Reaction of Catechol at the modified electrode surface [8].

## 2.2 Electrochemical Sensors

Electrochemical sensors are broad aspects of physical and analytical chemistry, material science biochemistry, solid-state physics, device fabrication, electrical engineering, and even statistical-analysis. A typical chemical sensor is a device that transforms chemical information in selective and reversible way, ranging from the concentration of specific sample component to composition analysis, into an analytically useful signal. This work, focus on electrochemical sensors from analytical perspective. A huge research effort has taken place over years to achieve electrochemical sensors with attractive qualities including rapid response, low cost, miniaturisable, superior sensitivity and selectivity, appropriate detection limits. Approximately 2000 peer-reviewed papers concerning electrochemical sensors were published in 2011 showing the considerable research effort underway in this field [1, 15].

The development of all voltammetric techniques has been based predominantly on the use of mercury, carbonaceous materials and noble metals as working electrodes. However, toxicity of mercury, and its limited range of potentials for mercury anodic reactions cause inconvenience in working with liquid mercury electrode. Carbon-based working electrode materials include all

---

allotropic forms of carbons graphite, glassy carbon, amorphous carbon, fullerenes, and nanotubes are all used as important electrode materials in Electroanalytical chemistry [1, 15].

Two branches of electrochemical sensors are developing:

- i. Sensors with increased specificity, and
- ii. Sensors capable of simultaneous/multiple determination [1].

The analytical and physical properties that must be considered when developing and commercializing chemical and biological sensors include (but are not limited to): Cost, Miniaturization, Sensitivity, Sensor reproducibility, Selectivity/Specificity, Multi-analyte detection, and Stability [1]

### **2.2.1 Chemically Modified Electrodes**

Chemically modified electrodes are different from other types of sensors as they are a molecular monolayer or micrometer-thick layers or films made from a certain chemical depending on the function of the electrode. The thin film is coated on the surface of the electrode (herein on a glassy carbon electrode). The outcome would be a modified electrode with special new properties in terms of physical, chemical, electrochemical, optical, electrical, (electron transport) and other useful properties [19]. Chemically modified electrodes depend on electron transport that is a general term for electrochemical process where the charge transports through the chemical film to the electrode. The term coverage is used to express the area-normalized in  $\text{mol/m}^2$  of a specific type of chemical site in the thin chemical film on the surface of chemically modified electrode [15, 20].

### **2.2.2 Purpose of Developing Chemically Modified Electrodes**

Advancement in the field of electrochemical sensors kept getting more thorough until chemists in this field found no use of bare surface to continue their investigations. The reason behind that is researchers that involved electrodes required certain chemical and physical properties that did not naturally exist in the materials used as electrical conductors (e.g. bare glassy carbon electrode). To solve their problem, they used chemical modification to tailor the materials they used. Atoms, molecules, and nano particles are attached to the surface of materials to modify their electronic and structural properties, leading to changing their functionality [20].

---

### 2.2.3 Applications of Chemically Modified Electrodes

In their first stage, CMSs were merely applied in technologies they were initially made for tuning surface for electrochemical investigations. After that, CMSs provided powerful routes to tune the performance of electrodes. The modification of sensors facilitated the following processes in Electroanalytical chemistry: Providing selectivity of electrodes, Resist fouling Concentrating species, Improving electrocatalytic properties, and Limiting of interference in samples [15].

### 2.2.4 Allotropes of Carbon

The three most important carbon based materials such as fullerene, carbon nanotubes and graphene are allotropes of carbon. These allotropes as illustrated in Figure 6 below have different dimensions; fullerenes, carbon nanotubes (CNTs), graphene, graphite and diamond have 0D, 1D, 2D and 3D structures respectively. Fullerenes are entirely composed of carbon in the form of spherical shape called Bucky balls, whereas carbon nanotubes have tubular arrangements. Currently, graphene is one of the hottest materials and it can be applied for electrochemical sensors and, numerous efforts were made to review the structure, preparation, properties and applications of graphene and its composite materials [21].

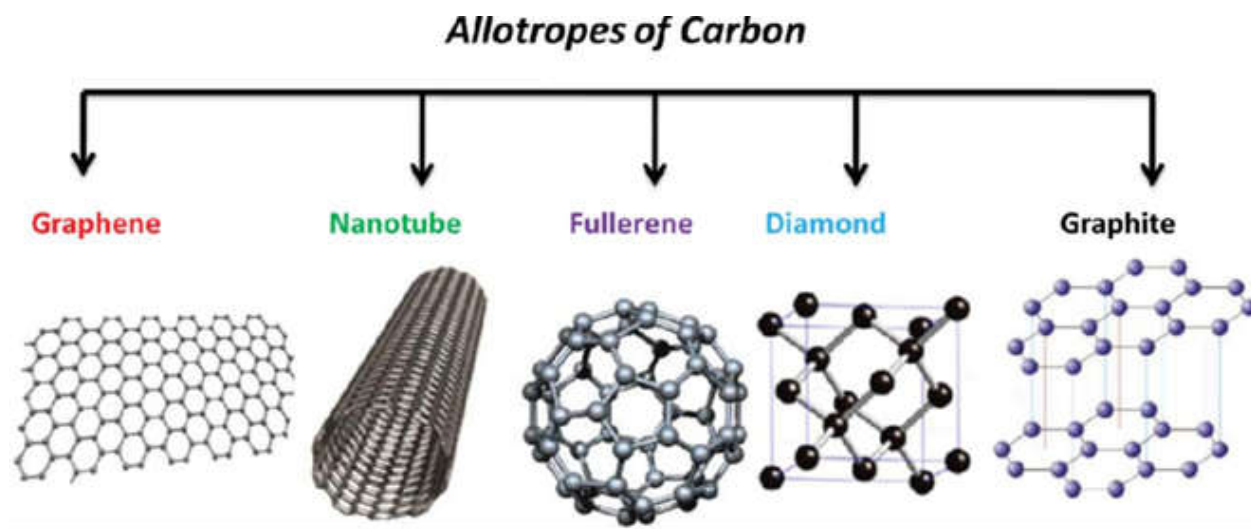


Figure 6: The allotropes of Carbon [22]

---

## 2.2.5 Carbon Nanotubes (CNTs)

The term “graphene” is sometimes used interchangeably with the term “carbon nanotubes” or CNTs see Figure 7 below. CNTs are sheets of graphene that have been rolled up into a nano-scale tube. The walls of the tube can be a single atom thick (SWCNT), or multiwall carbon nanotubes (MWCNTs) but the tube overall is more stable and less reactive with other substances than regular, linear graphene. Carbon nanotubes (CNTs), including single walled (SWCNTs) and multi-walled carbon (MWCNTs), have been used in various fields such as catalysis of redox reaction, nano electronics, electrochemical sensors, etc., due to their unique structure, electronic and mechanical characteristics. Sensors based on CNTs have received a lot of attention and have largely improved the voltammetric response (lower over voltages and higher peak currents) of variety of biological, clinical and environmental compounds [22]

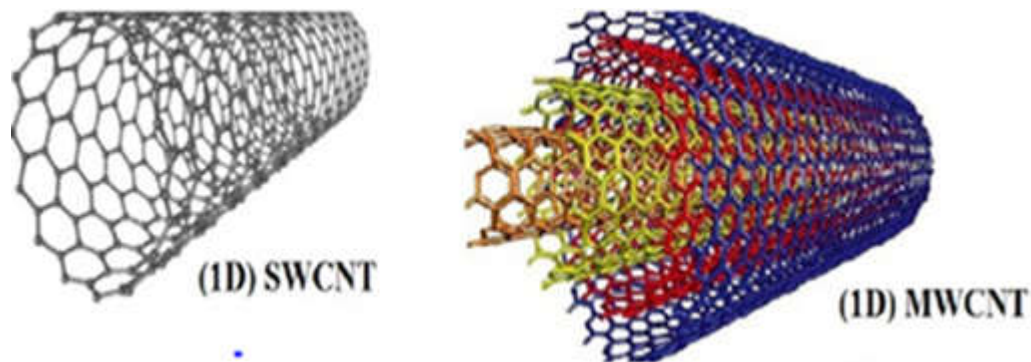


Figure 7: Schematic presentations of Carbon nano tubes

## 2.3 Graphene and Sensors

Graphene is a carbon allotrope that consists of flat monolayer  $sp^2$  carbon atoms bonded and arranged in honeycomb lattice. Since the discovery of graphene in 2004, this single atomic layer carbon material has gathered tremendous attention from researchers around the world because of its remarkable properties, such as surface area strong Young's modulus, good thermal conductivity, outstanding electrical conductivity, and optical transparency [17].

### 2.3.1 Structure of Graphene

The covalent bonds between nearest-neighbor carbon atoms in graphene which are  $sp^2$  hybridized orbitals Figure 8A, give graphene its extraordinary mechanical strength, making it possible to have free-standing graphene sheets, being only one atomic layer thick. The remaining  $p$ -electron per

---

atom is delocalized over the whole graphene lattice, and is responsible for the electrical conductivity of graphene. In un-doped graphene, the Fermi energy lies exactly at the Dirac: the  $\pi$ -band is completely filled, while the  $\pi^*$ -band is empty [24]. Structure of graphene can be viewed as Figure 8B below in terms of the structure of benzene. The 6 carbon atoms are situated at the corners of a hexagon and form covalent bonds with the H atoms. In addition to the 6 covalent  $\sigma$  bonds between the C atoms, there are three  $\pi$  bonds indicated by the doubled line. Graphene may be viewed as a tiling of benzene hexagons, as seen in Figure 8C where the H atoms are replaced by C atoms of neighboring hexagons and where the  $\pi$  electrons are delocalized over the whole structure [23].

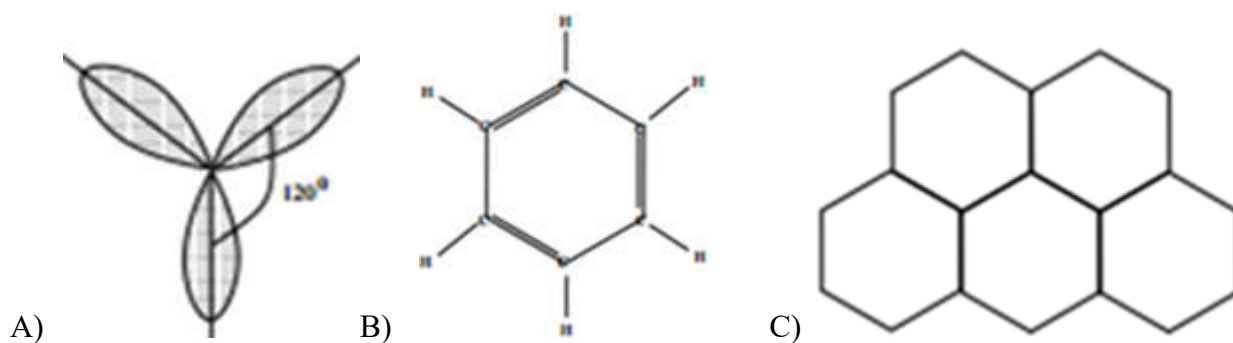


Figure 8: Structure of graphene: A) Schematic view of the  $sp^2$  hybridization. The orbital's form angles of  $120^\circ$ . B) Benzene molecule ( $C_6H_6$ ). C) Graphene where  $\pi$  electrons are delocalized over the whole structure [23].

### 2.3.2 Preparation of Graphene

Graphene has found its way into various applications, including energy conversion and storage (e.g., fuel cells and capacitors, sensors, electro-catalysts and electronic devices). Several approaches have been developed for the synthesis of graphene, such as mechanical cleavage, epitaxial growth, chemical vapor deposition, electrochemical exfoliation of graphite and reduction of graphene oxide (GO) that is derived from chemical exfoliation of graphite. Recently, non-covalent exfoliation of graphite by sonication in liquid phase has been reported. Of these approaches, the reduction of GO is regarded as one of the most promising routes for the mass production of graphene at a low cost and high yield, although only partially restore the properties of pristine graphene. The name given to this product is reduced graphene oxide (RGO), as it possesses properties that are different from pristine graphene [24].

---

## 2.4 Graphene Oxide (GO)

GO is typically derived from the chemical exfoliation of graphite oxide. GO is generally similar to graphite oxide in terms of its chemical structure, which contains plenty of oxygen functionalities on its carbon basal plane. However, the physical structure of GO is different from graphite oxide as the latter retains a stacked structure similar to that in graphite as seen in Figure 9.

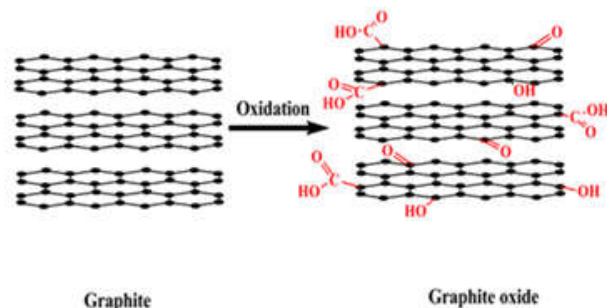


Figure 9: Schematic illustration of Oxidation of graphite [24]

In general, the GO is exfoliated into a single-layer or few-layered carbon sheets. The precise structure of GO remains under debate as the coverage of oxygen functionalities that exist on the GO varies widely with the different synthetic procedures. However, the generally accepted structural model of GO as shown in Figure 10, in which the hydroxyl and epoxy groups as dominant functional groups residing mainly on the basal plane of the GO sheets while the carbonyl and carboxyl groups accommodate the edges of the GO sheets [25].

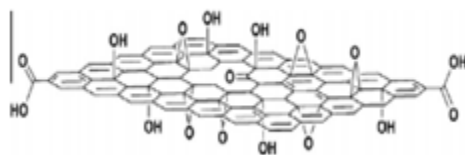


Figure 10: Chemical structural model of graphene oxide [25]

### 2.4.1 Preparation of Graphene Oxide

The first step in the synthesis of GO in a stable colloidal suspension begins with the oxidation of graphite to graphite oxide as in Figure 9. Subsequently, graphite oxide is exfoliated in the solution phase into individual GO sheets to form an aqueous GO colloidal suspension. Presently, the

---

Hummers and the modified version of this method are the most commonly used methods for the oxidation of graphite. All of these methods involve the oxidation of graphite in the presence of strong oxidants in acidic media. In Hummers' method, the graphite is oxidized using  $\text{KMnO}_4$  and  $\text{NaNO}_3$  in concentrated  $\text{H}_2\text{SO}_4$  to form graphite oxide. Kovtyukhova showed a modified version of Hummers' method to produce more heavily oxidized graphite, which involves pre-oxidation of graphite with  $\text{K}_2\text{S}_2\text{O}_8$  and  $\text{P}_2\text{O}_5$  in  $\text{H}_2\text{SO}_4$ . In another study, Marcano reported an improved method to synthesizing graphite oxide by the use of  $\text{KMnO}_4$  with a 9:1 ratio mixture of concentrated  $\text{H}_2\text{SO}_4$  and  $\text{H}_3\text{PO}_4$  [25].

The extent of graphite oxidation, which is typically quantified by the C/O atomic ratio, varies on the basis of the procedures used, reaction conditions and graphite precursor. The oxidation degree of graphite should be as low as possible because the single layer GO sheets are attainable using subsequent reduction processes. They demonstrated that the distance between the GO sheets did not increase when oxidation proceeded to a certain extent. The mildly oxidized GO could be produced by lowering the ratio of  $\text{KMnO}_4$  from 3:1 (Hummers method) to 1:1 during oxidation. The mildly oxidized GO has been reported to exhibit low defects, fewer oxygenated functionalities and a larger *p*-conjugated structure domain than those of the GO prepared by the typical Hummers' method [25].

The oxidation of graphite disrupts the  $\text{sp}^2$ -hybridized carbon network of the stacked graphene sheets in graphite and gives rise to defects and wider spacing between adjacent sheets as a result of oxygen functionalities on both sides of the carbon basal plane. It has been revealed that the distance between the adjacent sheets increases from 0.334 nm in graphite powder to 0.68 nm in graphite oxide powder. Owing to the hygroscopic nature of the stacked structure of GO sheets in graphite oxide, the intercalation of water molecules between the GO sheets readily occurs, as a result of ionization of the carboxylic groups and phenolic hydroxyl groups that exist on the GO sheets. The thickness of a single-layer GO sheet has been reported to be approximately 1–1.4 nm. The spacing between the GO sheets varies significantly, ranging from 0.6 nm to 1.2 nm depending on the relative humidity level within the stacked sheets. Thus, the increase in spacing between the sheets weakens the interaction between the sheets, which in turn facilitates the exfoliation of the graphite oxide into individual GO sheets upon sonication as illustrated in Figure 11 or mechanical stirring in water or polar solvent. However, several studies claimed that excessive ultrasonication could result

in a decrease in lateral dimension and hole defects. The individual GO sheets obtained from the exfoliation process consist mainly of single layer sheets or few-layer sheets that are readily dispersed in water to form a stable aqueous GO colloidal suspension. The stability of the aqueous GO colloidal suspension is believed to be attained through negative electrostatic repulsion  $\sim 1.4$  nm as a result of the introduction of oxygen functionalities on the carbon basal plane. In other words, it is approximately three times thicker than that of an ideal single layer graphene sheet [25].

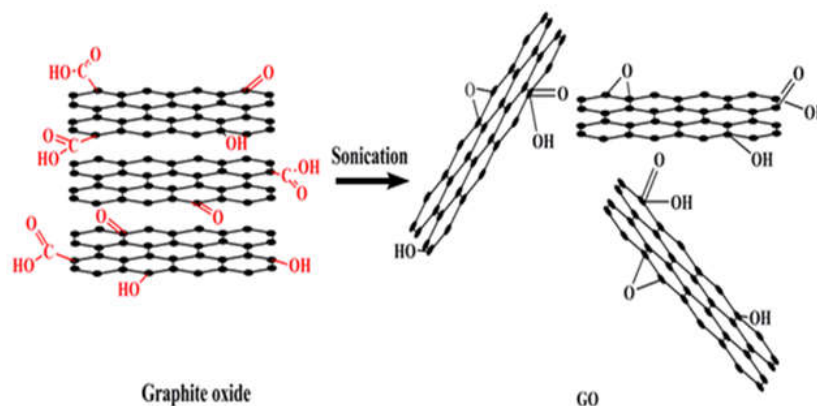
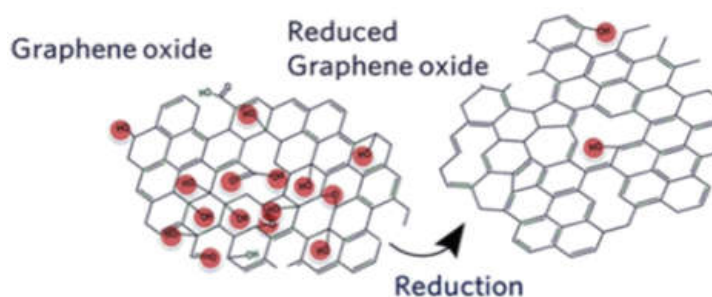


Figure 11: Chemical structure model of the graphite oxide and graphene oxide [24]

## 2.4.2 Synthesis of Electrochemically reduced Graphene oxide (ERGO)

As a result of impairment and disruption to the  $sp^2$  carbon bonding network arising from a plenty of oxygen functionalities on its carbon basal plane, GO is electrically insulating. Deoxygenation treatment of GO is required to restore the  $p$ -network, which in turn recovers the electrical conductivity of the resulting graphene materials. However, the resulting graphene material as seen in Figure 12 is not expected to exhibit the same electronic quality as that of pristine graphene as a result of residual oxygen functionalities and defects [24].



---

Figure 12: Chemical structure of graphene oxide, and reduced graphene oxide (RGO) [24]

The Deoxygenation of GO can be accomplished using chemical and electrochemical reduction techniques. The electrochemical reduction of GO can be carried out in two different routes as illustrated below.

### 2.4.2.1 One-step electrochemical Reduction Approach

In the one-step electrochemical approach, the GO sheets are directly electrochemically reduced from an aqueous colloidal suspension in the presence of buffer electrolyte to produce the ERGO thin films on an electrode surface. The electrochemical reduction process can be performed with cyclic voltammetry (CV), linear sweep voltammetry (LSV) at a constant potential mode in a standard three-electrode electrochemical system at room temperature. The electrochemical reduction is believed to take place when the GO sheets adjacent to an electrode accept electrons, yielding the insoluble ERGOs that attach directly onto the electrode surface. According to Liu, the electro deposition is driven by the difference in solubility between the GO and the resulting ERGO in the aqueous electrolyte solution [25].

Important parameters for the formation of high-quality films during the electrochemical reduction of GO from an aqueous suspension include [25]:

1. Selection of electrolyte: A phosphate buffer solution (PBS) is used as a supporting electrolyte with the GO colloidal suspension to form a medium in the one-step electrochemical reduction of GO. However, other electrolytes, such as NaCl and Na<sub>2</sub>SO<sub>4</sub>, can also be used as supporting electrolytes in GO.
2. Concentration of electrolyte: The concentration of the supporting electrolytes mixed with the GO colloidal suspensions should be very dilute. The concentration of the electrolyte is often correlated to the overall conductivity of the medium.
3. Conductivity: the optimal range was found to be between 4 and 25 mScm<sup>-1</sup> for neutral pH media (0.5 mg/ml GO and 0.25 M NaCl) at a reduction potential of 1.2 V with respect to SCE.
4. Appropriate pH: GO can be electrochemically reduced over a wide pH range of 1.5–12.5, Liu showed that the electrochemical reduction of GO at a pH higher than 10.0 failed to result in deposition of the ERGO films onto the electrode surface because the ERGO films

---

produced are soluble in strongly basic media and become unstable at pH values beyond 11.0 [25].

5. Constant potential: Electrochemical reduction of GO is commonly attained by applying a constant potential reduction or CV techniques. Linear sweep voltammetry (LSV) and differential pulse voltammetry (DPV) can also be used. A potential more negative than 1.5 V (vs. SCE) could lead to hydrogen gas bubble evolution from the reduction of water, creating a physical barrier that hinders the GO sheets from approaching the working electrode and completing the electrochemical reduction process.

#### 2.4.2.2 Two-step Electrochemical Reduction Approach

In the two-step electrochemical approach, which is the electrochemical reduction used in this work; a thin film of GO is first deposited onto the surface of an electrode, which acts as a substrate and is subsequently dried out to form a GO-coated electrode. The GO-coated substrate electrode is then subjected to electrochemical reduction using a standard three-electrode electrochemical system in the presence of a phosphate buffer as supporting electrolyte to produce ERGO films on the electrode substrate [25].

The GO film could be deposited or coated onto the surface of either insulating substrates (flexible plastic and glass) or conducting substrates (indium tin oxide, glass carbon or gold). However, the experimental setup for the electrochemical reduction of GO coated onto insulating substrate electrodes is slightly different from that of the GO coated onto conductive substrate electrodes, as illustrated in Figure 13 [25].

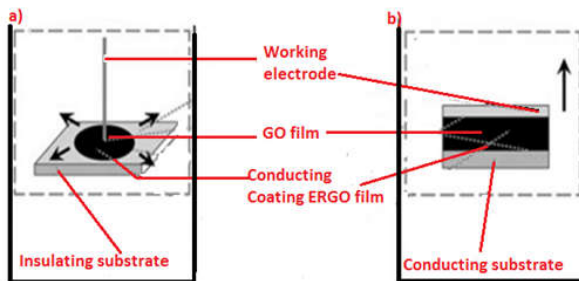


Figure 13: The electrochemical reduction of GO films coated on; a) insulating substrate and b) conductive substrate to ERGO film [25].

---

For the GO coated onto insulating substrate systems, an additional conductive electrode, such as glass carbon electrode, is required to be in contact with the GO-coated insulating substrate, which acts as the working electrode in the electrochemical cell. In contrast, for the GO coated directly on conductive substrate systems, the GO-coated conductive substrate acts concurrently as a working electrode in the electrochemical cell without the need of additional conductive electrodes. The parameters of ERGO in the two-step electrochemical reduction include [25]

1. The supporting electrolytes: the phosphate buffer solution (PBS) has been widely used as a supporting electrolyte other supporting electrolytes such as KCl, KNO<sub>3</sub>, and NaCl have also been reported. Electrochemical reduction takes place in an acidic or near neutral pH electrochemical medium.
2. Constant potential reduction technique: The selection of the applied cathodic reduction potential is based on the cathodic peak potential observed in the cyclic voltammogram. The cathodic peak potential for the reduction of GO is influenced by the pH value of the buffer medium.
3. The electrochemical reduction of GO to ERGO is an irreversible process. The reduced GO-coated electrode relies on the selection of the appropriate cathodic reduction potential and time.

The electrochemical reduction of GO is accomplished through removal of oxygen functionalities in the GO, which in turn recovers the graphitic network of the  $sp^2$  carbon bond in the resulting ERGO. Complete removal of oxygen functionalities in the GO to fully recover the unique properties of pristine graphene currently is still beyond reach. However, the oxygen content of the resulting ERGO can be modulated by changing the electrochemical reduction time and cathodic potential in the constant potential technique versus Ag/AgCl or SCE. We can summarize the one and two step electrochemical reduction of graphene oxide as in Figure 14 below [25].

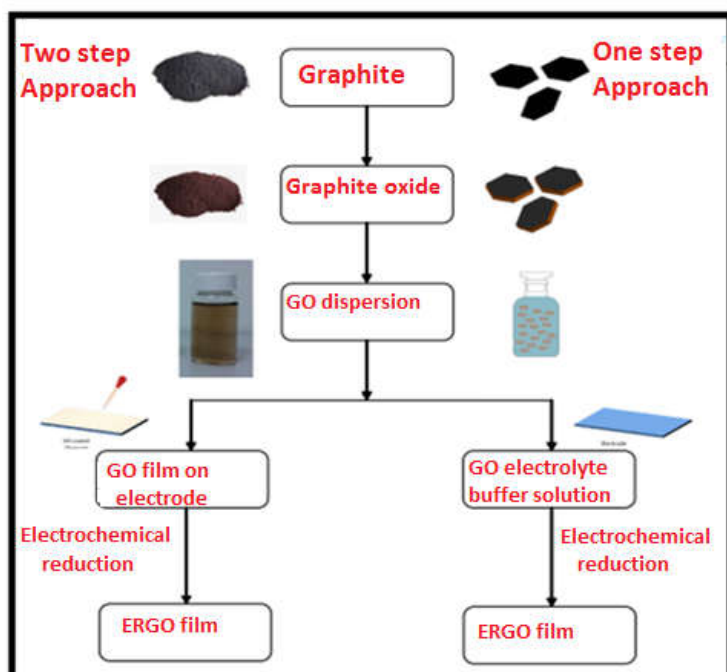


Figure 14: Schematic illustration of electrochemical reduction approach for production of ERGO [25]

### 2.4.5 Advantages of ERGO Compared to CRGO

The mass production of graphene's can also be achieved by chemical reduction of graphene oxides (GO) with various kinds of reducing agents, however, the electrochemical approach has several clear advantages over the chemical approach. The electrochemical approach is relatively economical, fast and environmental friendly (non toxic) method to produce graphene whereas the chemical method uses toxic and hazardous chemicals such as hydrazine or dimethylhydrazine in the chemical reduction process. Thus, the resulting graphenes are free from contamination arising from the residue or excess toxic and hazardous reducing chemicals that exist in the solution. Apart from that, electrochemical approach offers a more controllable and effective way for the reduction of oxygen functionalities by simply adjusting the electrode potentials. The chemical approach may require more than one reducing agents or steps to achieve effective reduction of oxygen functionalities of the GO to the same extent. Moreover, the resulting graphene also tend to agglomerate upon reduction in liquid phase. Conversely, electrochemical approach may produce graphene directly onto the electrode substrates which could be used for specific applications, such as biosensor and electrocatalysis without further steps or treatments [25].

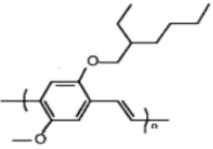
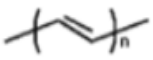
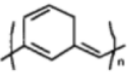
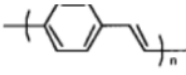
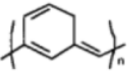
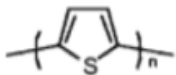
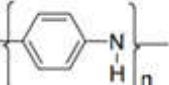
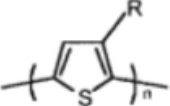
## 2.5 Conducting Polymers (CPs)

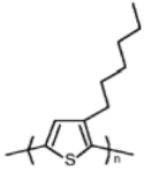
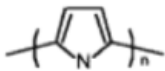

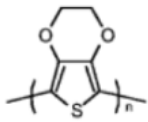
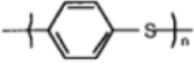
Polymers have long been known as insulating materials and are often used to insulate cables and electrical devices. However, there are also a number of polymers that are electrically conductive. A few intrinsically conducting polymers(ICPs) exist that have alternating single and double bonds along the polymer backbone (conjugated bonds) or that are composed of aromatic rings such as phenylene, naphthalene, anthracene, pyrrole, and thiophene which are connected to one another through carbon-carbon single bonds[ 26].

Conjugation means that the polymer backbone consists of alternating single and double bonds. The strong chemical bonds between the carbon atoms are the so-called localized  $\sigma$  bonds, whereas the double bonds provide weaker and less strongly localized  $\pi$  bonds [26].

Some examples of molecular structures of conjugated polymers with their repeating monomer are given in Table1 below.

Table 1 Molecular structures of some conjugated polymers and their repeating unit [26].

Conjugated Polymer	Repeating Monomer	Conjugated Polymer	Repeating Monomer
Alkoxy- substituted Poly Para-phenylene (MEH-PPY)		Polyacetylene (PA)	
Polyheptadiyne (PHT)		Polyphenylene vinylene(PPV)	
Polyaniline (PANI)		Polythiophene (PT)	
Polyaniline (PANI)		Poly (3 – alkyl) thiophene (P3AT) ( R-methyl, butyl- etc)	

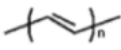
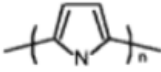
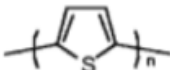
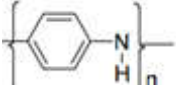
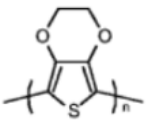
Poly (3-hexy) thiophene (P3HT)		Polypyrrole (PPy)	
Polyparaphenylene (PPP)		Polyethylene dioxythiophene ( PEDOT )	
Polyparaphenylene sulphide ( PPS )			

However, the conductivity of these polymers is rather low. When an electron is removed from the valence band by oxidation (p-doping) or added to the conducting band by reduction (n-doping) does the polymer become highly conductive. Through such a doping process, charge defects (polaron, bipolaron and soliton) are created that can travel through the backbone of the polymer, or to be more specific, through the conduction band. The four main methods of doping are [26, 27]:

- I. Redox p-doping: Some of the  $\pi$ -bond are oxidized by treating the polymer with an oxidizing agent such as iodine, chlorine, arsenic pentafluoride --- etc.
- II. Redox n-doping: Some of the  $\pi$ -bonds are reduced by treating the polymer with reducing agents such as lithium, and sodium naphthaline.
- III. Electrochemical p- and n-doping: doping is achieved by cathodic reduction (p) or anodic oxidation (n).
- IV. Photo-induced Doping: The polymer is exposed to high energy radiation that allows electrons to jump to the conduction band. In this case, the positive and negative charges are localized over a few bonds

Some of the conducting polymers with their possible doping materials are given in Table 2.

Table 2 Structures and doping chemicals of some common conducting polymers [9]

Polymer	Structure	Doping materials
Polyacetylene		$I_2, Br_2, Li, Na, AsF_5$
Poly pyrrole		$BF_4^-, ClO_4^-$
Polythiophene		$BF_4^-, ClO_4^-$
Polyaniline		$BF_4^-, ClO_4^-$
Polyethylene dioxythiophene		$BF_4^-, ClO_4^-$

Electrical conductivity of polymers can be classified as [28]:

Electronic Conduction by electrons (n-type), and this can be intrinsic and extrinsic (impurities donate electrons. The conduction by holes (p-type) intrinsic and extrinsic (impurities accept electrons). Metallic type conduction rare in polymers; polythiazyl  $(-SN-)_n$  is one example.

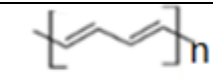
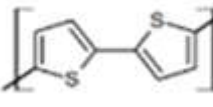
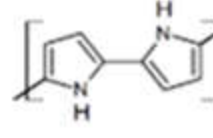

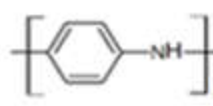
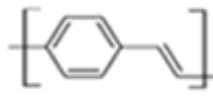
Ionic: electrolytic (cationic, anionic, ambipolar) intrinsic (self dissociating) extrinsic (impurities or dopants). Protonic for example in Nylon 66 and poly (ethylene oxide) [29].

In general conducting polymers can be electron-conducting polymers, proton - conducting polymers, and ion- conducting polymers [28 29].

Proton conduction can be observed in many materials, from rigid inorganic oxides at high temperatures to flexible organic polymers at room temperature, leveraging different conduction mechanisms. Depending on the type of proton conductor, proton-conducting polymer electrolytes can be classified into different groups, as follows: system with strong hydrogen bonding; diffusion or vehicle mechanism in a system with weak hydrogen bonding; and direct transport via polymer chain segmental motion [29].

Polymeric proton-conducting electrolytes possess “intrinsic” proton conductivity from the functional group in the polymer chains, whereas the inorganic/polymer proton-conducting electrolytes blend inorganic proton conductors with a polymeric matrix to form gels or composites. Table 3 below lists typical conductivities of some common conjugated polymers and their repeating units. The actual conductivity not only depends on the structure and morphology of the polymer but also on the type of dopant and its concentration [29].

Table 3 Electrical Conductivity of Some Conjugated Polymers[30]

Conjugated Polymer	Repeating Unit	Conductivity (Scm <sup>-1</sup> )
Trans Polyacetylene		10 <sup>3</sup> -10 <sup>5</sup>
Polythiophene		10 <sup>3</sup>
Polypyrrole		10 <sup>2</sup> – 7.5 -10 <sup>3</sup>
Poly (p-phenylene)		10 <sup>2</sup> -10 <sup>3</sup>
Polyaniline		2- 10 <sup>2</sup>
Poly(p-Phenylene vinylene)		- 10 <sup>2</sup>

## 2.6 Bromocresol Purple

IUPAC name is 4, 4-(1,1-Dioxido-3H-2,1-benzoxathiol-3,3-diyl)-bis(2-bromo-6-methylphenol). Other name 5',5''- Dibromo-*o*-cresolsulfonephthalein or bromocresol purple is with molecular formula C<sub>21</sub>H<sub>16</sub>Br<sub>2</sub>O<sub>5</sub>S, and structural formula as in figure 15 below.

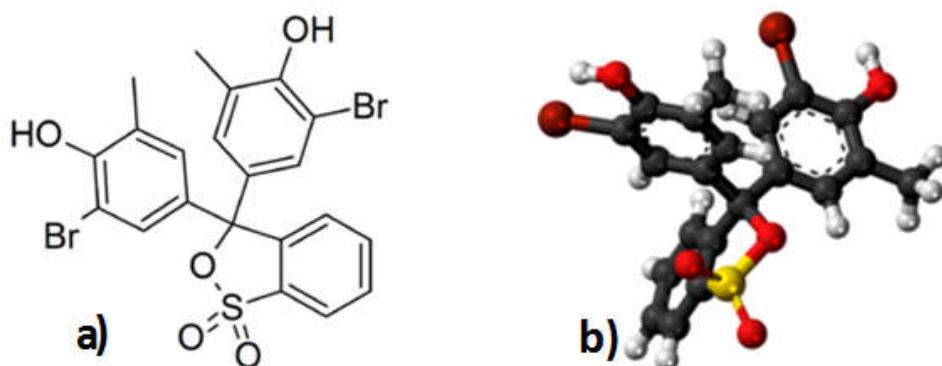
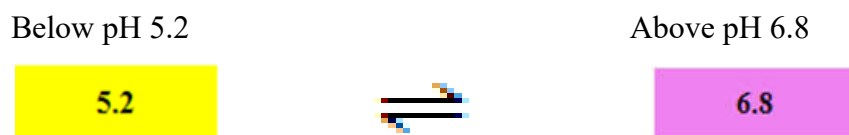


Figure 15: a) Molecular structure of bromocresol purple. b) 3D structure

Bromocresol purple (BCP), 5, 5-dibromo-o-cresolsulfophthalein is a pH indicator [31].



It is also used as dye to measure albumin in medical laboratories. The mechanism for the color change in bromocresol purple bound to human serum albumin is a reversible redox reaction as in Figure 16 below [32].

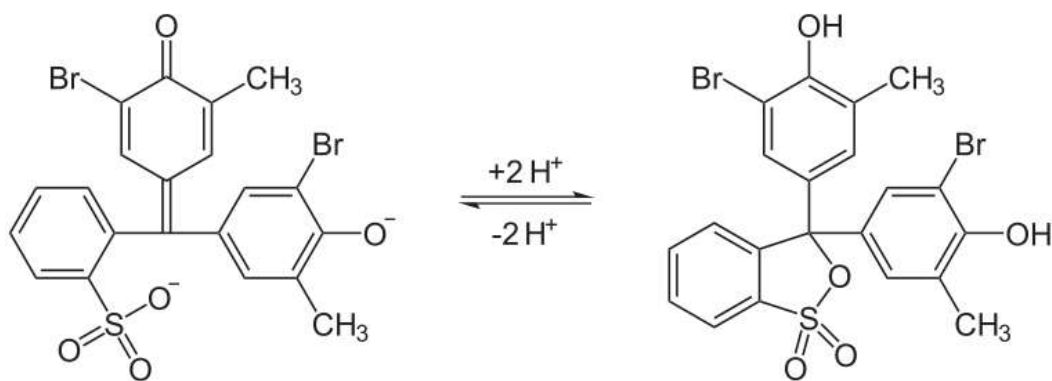


Figure 16 Reversible redox reaction of BCP [33]

Its electropolymerization at the electrode surface and its function as an electrocatalyst have been reported in some literature for some phenolic compounds. In this work, a polymer film of BCP is used to modify electrochemically reduced graphene oxide on glassy carbon electrode (GCE) and

---

described the electrochemical behaviors of CC at the poly (BCP) modified glassy carbon electrode. The poly (BCP) modified electrode possessed conjugated bonds, and a great deal of active sites and better conductivity, which led to the dissimilar conjugation effect of the purine derivatives with the electrode interface. Therefore, the electrochemical reversibility of the oxidation of CC may be greatly improved in the presence of the poly BCP film by accelerating the rate of electron transfer, which indicated that the poly BCP film is first reduced by oxidizing CC and then oxidized when CC is reduced [32, 33].

## **2.7 The Electrochemical Cell**

The electrochemical cell, where the voltammetric experiment is carried out, consists of a working (indicator) electrode, a reference electrode, and usually a counter (auxiliary) electrode. In general, an electrode provides the interface across which a charge can be transferred or its effects felt. Because the working electrode is where the reaction or transfer of interest is taking place, whenever we refer to the electrode, we always mean the working electrode. The reduction or oxidation of a substance at the surface of a working electrode, at the appropriate applied potential, results in the mass transport of new material to the electrode surface and the generation of a current. Even though the various types of voltammetric techniques may appear to be very different at first glance, their fundamental principles and applications derive from the same electrochemical theory [34, 35].

### **2.7.1 The Working Electrode**

Definition - What does Working Electrode mean? The working electrode is at which the investigation process occur. The working electrode can be bare or coated. Usually in the range of positive potential, platinum, gold, and carbon (graphite, glassy carbon) electrodes are used. The working electrode can be referred to as either cathodic or anodic [35].

### **2.7.2 The Function of the Working Electrode**

A fixed potential difference is applied between the working electrode and the reference electrode. This potential drives the electrochemical reaction at the working electrode's surface. The current produced from the electrochemical reaction at the working electrode is balanced by a current flowing in the opposite direction at the counter electrode. The reference electrode acts as a

---

reference point for the redox couple. The current resulting from the electrochemical reaction is amplified and, when plotted as a function of time, appears as a peak on the recording device [35].

### **2.7.3 Selection of Working Electrode**

The selection of a working electrode material is critical to experimental success. Several important factors should be considered [36, 37].

- 1) The material should exhibit favorable redox behavior with the analyte, ideally fast, reproducible, fast electron transfer without electrode fouling.
- 2) The potential window over which the electrode performs in a given electrolyte solution should be as wide as possible to allow for the greatest degree of analyte characterization.
- 3) The cost of the material should be cheap.
- 4) Its ability to be machined or formed into useful geometries.
- 5) The ease of surface renewal following a measurement, and
- 6) Toxicity that is, it should be non toxic.

### **2.7.4 Types of Working Electrodes**

A wide variety of working electrodes are available for use. The most common working electrode materials utilize carbon. Originally the carbon paste electrode was developed, but this was soon replaced by more convenient and stable carbon-based working electrodes including those made from glassy carbon, modified glassy carbon, pyrolytic carbon and porous graphite. Metals such as platinum, gold, silver, nickel, mercury, gold amalgam and a variety of alloys are now also commonly used as working electrode materials [35].

### **2.7.5 Glassy Carbon Electrode**

Owing to excellent physical and chemical properties, glassy carbon electrodes have been widely used in Electroanalytical chemistry. Electrochemical behaviors of GCE are associated with the composition and structure of the surface. However, the bare GCE shows low-activity for some reactions, because of the poor surface state of the electrode. In order to improve the performance of the surface of electrodes, various surface treatments have been studied to date, such as mechanical polishing, heating, electrochemical oxidation, laser activation, exposure to UV generated ozone and

---

photo catalytic pretreatment. Among these methods, electrochemical modification is the most extensively studied one due to its good reproducibility and easy operation, and the electron transfer rate or adsorptive behavior of the GCE for some electro active analytes is largely increased with modification. Figure 17 shows image of common glassy carbon electrode [34, 37].



Figure 17: Image of glassy carbon electrodes

### 2.7.6 Modified Electrodes

The rate of electron transfer across an electrode/solution interface is dependent on the physical and chemical properties of the electrode surface. Control of reactivity of the electrode/solution interface, if achieved, can influence the process of electrocatalysis. One variable which has been commonly used for controlling reaction at the surface is the applied potential. The other ways of controlling the electrochemical processes is the modification of the electrodes [36, 37].

Modified electrodes accelerate electrode reactions that are kinetically hindered on the bare electrode surface. A charge transfer occurs between the attached mediator and the dissolved analyte in an unhindered redox reaction. Polymer-modified electrodes are prepared either by casting polymer solution on the solid electrode surface and allowing the solvent to evaporate or by electro polymerization of a monomer. The polymer film is either an electronic insulator, but an ionic conductor, or a mixed electronic and ionic conductor. The first type of films is used for the preparation of perm- selective coatings that serve to prevent unwanted matrix constituents reaching the electrode surface. Electrochemical reactions in mixed conductor films depend on physicochemical processes, such as, the transport of ions within the polymer phase, the distribution of redox states in the polymer and electronic charge transfers between them, as well as heterogeneous charge transfer between the electrode and the polymer film [35].

---

## 2.8 General Theory of Cyclic and Differential Pulse Voltammetry

### 2.8.1 Voltammetric Sensing Principles

What are voltammetric techniques?

The term voltammetry is derived from voltamperometry, and it expresses that the current is measured as a function of voltage, i.e., electrode potential. Although an electrochemical cell needs only two electrodes to operate, it is very important to introduce a third electrode for voltammetric techniques. One of these electrodes is a reference electrode, i.e., an electrode which has a known and fixed electrode potential. No current should ever pass this electrode, as a current would change its potential, and possibly damage this electrode. The reference electrode is used to control the potential of the working electrode by measuring the voltage between these two electrodes. A cell consisting of a working electrode (WE), an auxiliary electrode (AE) and a reference electrode (RE) is called a three-electrode cell [38].

Depending on the exact mode of signal transduction, electrochemical sensors can use a range of modes of detection such as potentiometric, voltammetric and conductmetric. Each principle requires a specific design of the electrochemical cell. Voltammetry provides an Electroanalytical method, the premise of which is that current is linearly dependent upon the concentration of the electro active species (analyte) involved in a chemical or biological determination process (at a scanned or fixed potential). Voltammetry implies a varying voltage. Cyclic voltammetry, differential pulse, square wave and stripping voltammetry are some of the most common techniques [35].

In voltammetry, the effects of the applied potential and the behavior of the redox current are described by several well-known laws. The applied potential controls the concentrations of the redox species at the electrode surface ( $C_O^0$  and  $C_R^0$ ) and the rate of the reaction ( $k^0$ ), as described by the Nernst or Butler–Volmer equations, respectively. In the cases where diffusion plays a controlling part, the current resulting from the redox process (known as the faradic current) is related to the material flux at the electrode–solution interface and is described by Fick’s law. The interplay between these processes is responsible for the characteristic features observed in the voltammogram of the various techniques [38].

---

Voltammetry is the general term for all techniques in which the current is measured as a function of electrode potential. At the beginning of its development was Jaroslav Heyrovsky', the inventor of a voltammetric technique which he named POLAROGRAPHY. (The term polarography was meant to indicate that the polarization of an electrode was graphically recorded as current–potential curves: current-flow means depolarization, and no-current-flow means polarization, meaning that the potential increases without or only with a minor current response). The molecules or ions are oxidized or reduced at electrodes. The generation of faradic currents needs the molecules or ions to reach the electrode surface. This can be accomplished only by mass transport toward the electrode surface. There are only three possible mechanisms which can transport them diffusion in a concentration gradient, migration of ions in a potential gradient, and convection. A concentration gradient will always build up at the electrode/electrolyte interface, when the compound is oxidized or reduced at the electrode surface [39].

The (Nernst) diffusion layer thickness  $d_{\text{Nernst}}$  is the distance from the interface to the intercept of the two (almost) linear parts of the concentration profile. The diffusion profile depends on the diffusion coefficients of diffusing ions (or molecules), and it is a function of time. The diffusion layer thickness grows with time, and the concentration gradients (i.e., the steepness of concentration versus distance function) will decrease with time. The diffusion profile also depends on the electrode geometry and size [38].

## **2.8.2 Electrochemical Reversibility and Irreversibility**

For an electrode reaction to proceed, the reactant has to be transported to the interface, and the product has to be transported away from the interface as shown in Figure 18.

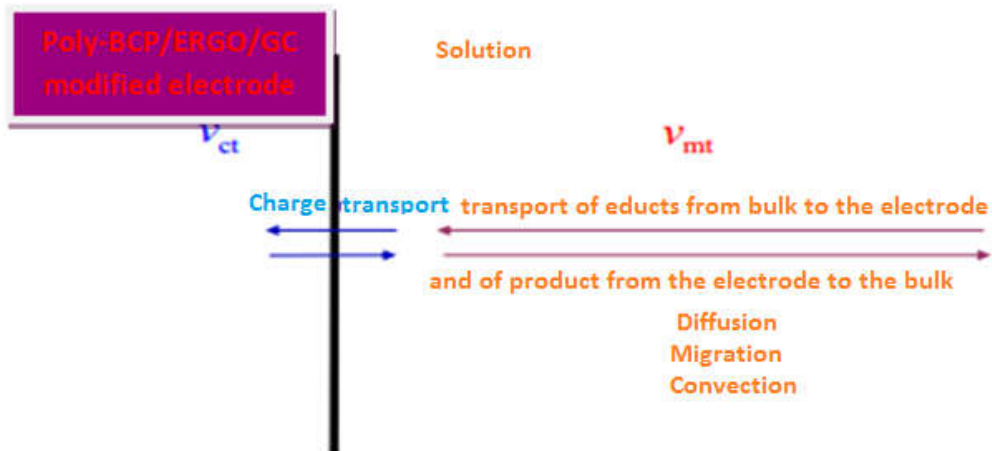


Figure 18: The rate of charge transfer  $v_{ct}$ , and the rate of mass transport  $v_{mt}$  of an electrode reaction [40]

At the interface, the charge transfer occurs with the rate  $v_{ct}$ . The overall rate of the electrode reaction can be limited [38]:

- By the mass transport of reactant and products to/from the electrode,
- By the rate of charge transfer

When the equilibrium between the oxidized and reduced forms of the electro active compound is very quickly established at the interface, i.e., when  $v_{ct}$  is faster than  $v_{mt}$ , the ratio  $\left(\frac{a_{Ox}}{a_{Red}}\right)_{Interface}$  at the interface will assume exactly the value which follows from the Nernst equation for this potential.

$$E_{A/B} = E^O + \frac{RT}{nF} \ln \left( \frac{a_{Ox}}{a_{Red}} \right)_{Interface} \text{----- (1)}$$

The Nernst equation describes an equilibrium situation, and hence a system where the ratio  $\left(\frac{a_{Ox}}{a_{Red}}\right)_{Interface}$  corresponds to the potential given by the Nernst equation, is called an electrochemically reversible one. However, when the charge-transfer rate  $v_{ct}$  is smaller than the mass transport rate  $v_{mt}$ , the equilibrium cannot be established with a sufficient rate and the ratio of

$\left(\frac{a_{Ox}}{a_{Red}}\right)_{Interface}$  at the interface will deviate from the ratio given by the Nernst equation for this potential. Then the electrochemical system has to be regarded as irreversible. One can phrase this also as follows: the current is the observable which tells us that how an electrochemical reaction proceeds, that is if that current is smaller than expected, the reaction is obviously not proceeding at equilibrium and thus not reversible. Figure 19 illustrates this using a rate scale.

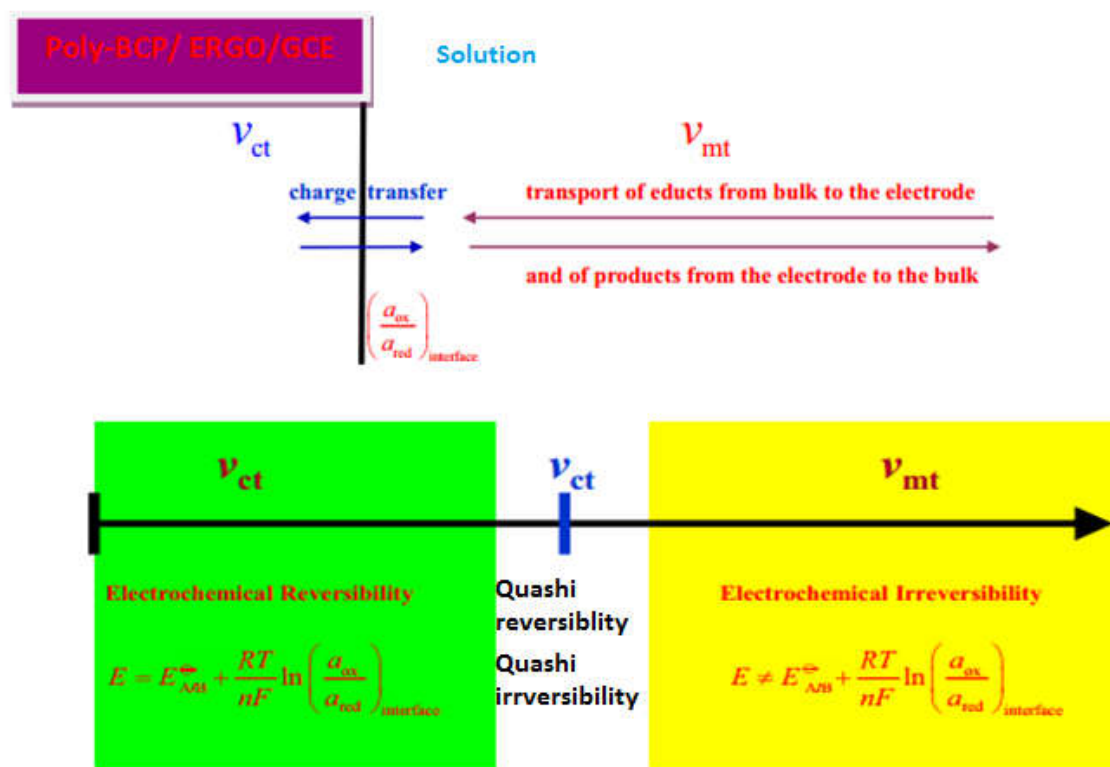


Figure 19: The relation of the rate of charge transfer  $v_{ct}$  to the rate of mass transport  $v_{mt}$  for a reversible electrochemical system [38].

For voltammetric analysis, it is important to note that the rate of charge transfer  $v_{ct}$ , and the rate of mass transport  $v_{mt}$  can be, in certain limits, changed by purpose. The transport rate can be changed by the hydrodynamic conditions (rate of stirring the solution, rate of rotating the electrode, drop time of the DME (Dropping mercury electrode) ... etc. From this follows that the characterization of an electrochemical system as reversible or irreversible, is nothing absolute, but it depends on the experimental conditions [40].

### 2.8.3 Cyclic voltammetry

Cyclic voltammetry is the most widely used technique for acquiring qualitative information about electrochemical reactions. It offers a rapid location of redox potentials of the electro active species. In cyclic voltammetry, one sweeps the potential of the working electrode at a specific sweep rate (in volts / sec), and measures the resulting current vs. time curve Figure 20. Usually the sweep is reversed at a specific switching potential, hence the name cyclic voltammetry [39].

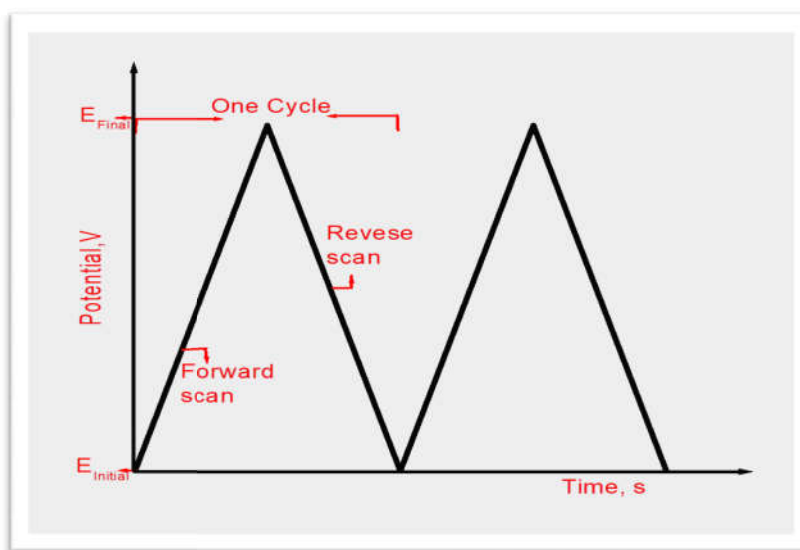


Figure 20: Potential –time excitation signal in cyclic voltammetric experiment [39].

Since the sweep rate is constant and the initial and switching potentials are known, one can easily convert time to potential, and the main purpose is to record current vs. applied potential. Figure 21 illustrates these concepts. The resulting current vs. applied potential curve (a cyclic voltammogram) is predicted for an ideal, reversible system to have the shape shown in Fig 21. When the potential of the working electrode is more positive than that of a redox couple presents in the solution, the corresponding species is oxidized (i.e. electrons going from the solution to the electrode) and produce an anodic current. Similarly, on the return scan, as the working electrode potential becomes more negative than the reduction potential of a redox couple, reduction (i.e. electrons flowing away from the electrode) causing to occur a cathodic current [39].

What are the notations in figure 21 mean? For the forward scan (a: onset potential) the current is first observed to peak at (b, Peak Potential)  $E_{pa}$  (with value  $i_{pa}$ ) indicating oxidation of species and

then drops (c: Switching potential) due to depletion of the reducing species from the diffusion layer, and for the reverse scan current is observed to peak at (e: Peak Potential)  $E_{pc}$  (with value  $i_{pc}$ ). Providing that the charge-transfer reaction is reversible, that there is no surface interaction between the electrode and the reagents (f: offset potential), and that the redox products are stable at least in the time frame of the experiment [38, 39].

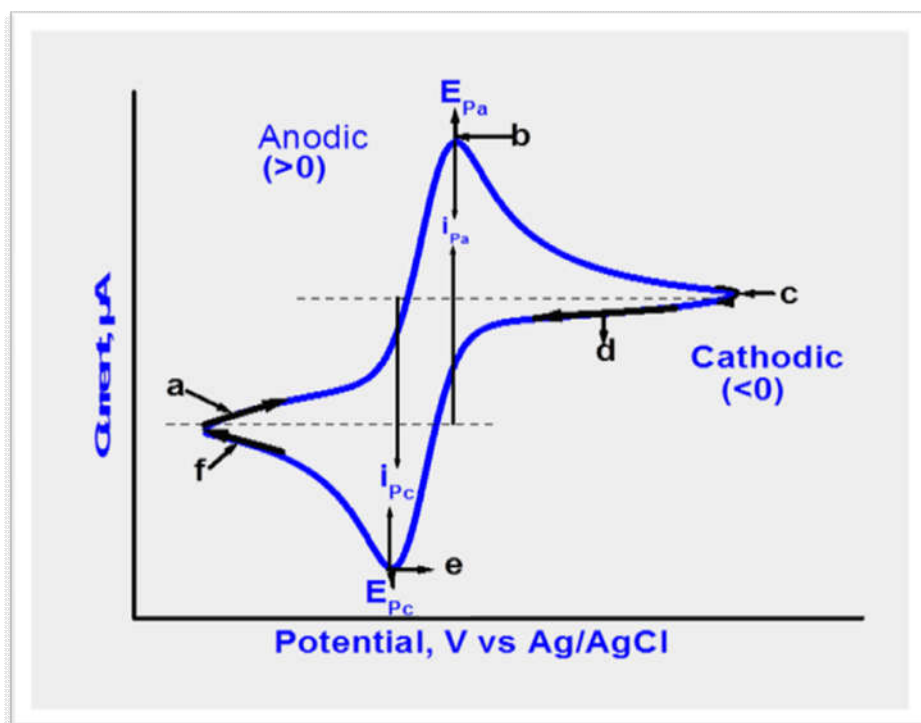


Figure 21: A cyclic voltammogram [39]

The peak current  $i_p$  of a reversible system is described by the Randles Sevcik equation for the forward sweep of the first cycle [38]

$$i_p = (2.69 \times 10^5) n^{3/2} A D^{1/2} \nu^{1/2} C \text{-----} (2)$$

Where  $i_p$  is the peak current in  $A$ ,  $n$  the number of electron in the redox reaction,  $A$  the electrode surface area in  $cm^2$ ,  $D$  is the diffusion coefficient in  $cm^2 s^{-1}$ ,  $C$  the concentration in  $mol cm^{-3}$ , and  $\nu$  the scan rate in  $V s^{-1}$ .

The midpoint potential of the two peaks in the voltammogram is given by:

$$E_{mid-point} = \frac{E_{Pa} + E_{Pc}}{2} = E^0 + \frac{RT}{nF} \ln \left( \frac{D_R^{1/2}}{D_O^{1/2}} \right) \text{-----(3)}$$

Where  $E^0$  is the redox potential, and  $D_O$  and  $D_R$  are the diffusion coefficients for the oxidized and reduced halves of that couple. It is frequently reasonable to assume that  $D_O$  and  $D_R$  are nearly equal, and in such a case the midpoint potential is very nearly equal to the redox potential. In other words a cyclic voltammogram can quickly show the presence of all species that undergo oxidation reduction reactions at the working electrode within the limits set by a redox couple in which both species rapidly exchange electrons with the working electrode is termed an electrochemically reversible couple. The formal potential  $E$ , centered between  $E_{Pa}$  and  $E_{Pc}$  [39]

$$E = \frac{E_{Pa} + E_{Pc}}{2} \text{-----(4)}$$

Finally, the separation between the two peaks of the voltammogram is given by:

$$\Delta E = |E_{Pa} - E_{Pc}| = 2.3 \frac{RT}{nF} = \frac{59}{n} \text{mv} \text{-----(5)}$$

The number of electrons ( $n$ ) transferred in the electrode reaction is determined from the separation between the peak potentials:

$$E = \frac{E_{Pa} + E_{Pc}}{n} \text{-----(6)}$$

For a reversible electrode reaction the ratio of  $i_{Pa} / i_{Pc}$  is one, difference in peak potential for two electron transfer is 29 mV,  $i_{Pa}$  increases with  $v^{1/2}$  and is directly proportional to concentration.

For an irreversible process, i.e. is slow (sluggish) electron transfer at the electrode surface, the ratio of  $i_{Pa} / i_{Pc}$  is greater than one, the peak current is given by

$$i_p = 2.69 \times 10^5 (n_a \alpha)^{1/2} A C D^{1/2} v^{1/2} \text{-----(7)}$$

Where  $n_a$  is the number of electrons in the rate determining steps, and  $\alpha$  is transfer coefficient. All other quantities have the same meaning as equation (2). In the case of a totally irreversible reaction only the peaks on the forward scan is observed. Irreversibility is due to slow electron transfer rate.

Hence, depending on what is already known about a given system, one could determine the concentration, the diffusion coefficient, the number of electrons per molecule of analyte oxidized or reduced, and/or the redox potential for the analyte, all from a single experiment [38].

## 2.8.4 Differential Pulse Voltammetry

A potential wave form for differential pulse voltammetry (DPV) is shown in Figure 22. The DPV technique is mainly used in electro analysis, just one drop or a solid electrode is used to obtain a voltammogram. The importance of DPV in chemical analysis is based on its superior elimination of the capacitive/background current. This is achieved by sampling the current twice: once before pulse application and then at the end of the pulse. The output from the potentiostat/voltammograph is equal to the difference in the two current values [40].

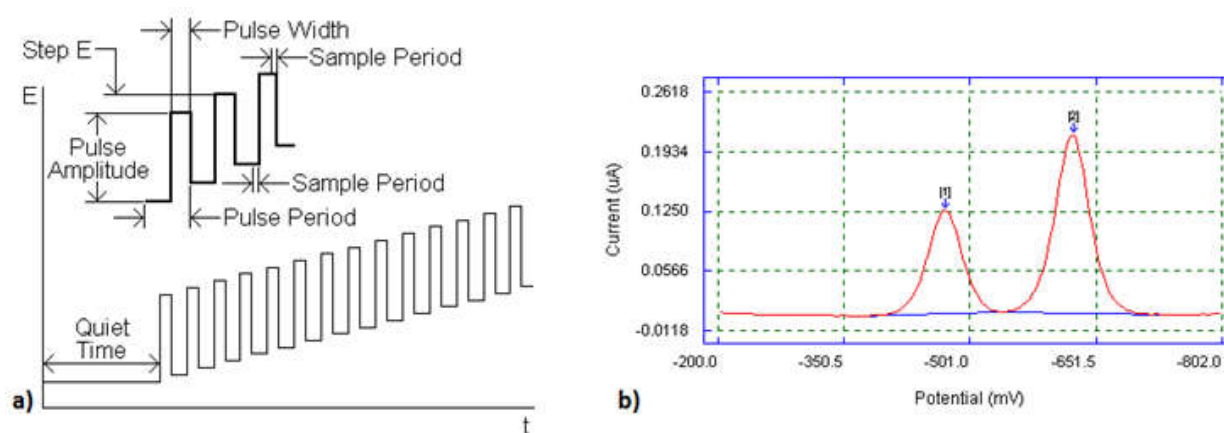


Figure 22: Differential Pulse Voltammetry a) an anodic scanning of the potential vs time; b) Plot of voltammogram [40]

The double current sampling allows the analyst to detect the analytes present in the solution at a concentration as low as  $0.05 \mu\text{M}$ . Another consequence of double sampling is that the differential pulse voltammogram are peak-shaped. For a reversible system, the peak height,  $i_p$ , of a differential pulse voltammogram is Potential, which can be written as  $E_p$

---


$$\Delta i_p = \frac{nFAD_{Ox}^{1/2}C^*}{\pi^{1/2}t_p^{1/2}} \left( \frac{1-\delta}{1+\delta} \right) \text{-----(8)}$$

where  $\sigma = \exp nFE_p/2RT$  . As  $E_p$  decreases, the quotient  $(1 - \sigma) / (1 + \sigma)$  diminishes and finally reaches zero. Due to double sampling of the current, the peak potential,  $E_p$ , precedes the formal

$$E_p = E_C^0 + \frac{RT}{nF} \ln \left( \frac{D_{Red}}{D_{Ox}} \right)^{1/2} - \frac{\Delta E_p}{2} \text{-----(9)}$$

The peak width at half height,  $w_{1/2}$ , for small values of  $E_p$  turns out to be

$$w_{1/2} = 3.52 \frac{RT}{nF} \text{-----(10)}$$

which gives, for 25°C and n =1, 2, and 3, the values of 90.4, 45.2, and 30.1 mV, respectively [39].

### 2.8.5 The supporting electrolyte

Limitation of migration is achieved by screening the electrode using a supporting electrolyte, meaning a solution which ions do not discharge themselves at the electrode in the experimental conditions. This electrolyte is added at high concentration to the sample and could be a simple salt, acid, base, a buffer solution or a chelating reagent. The supporting electrolyte surrounds the electrode with ions having the same charge of the depolarizing agent, reducing in this way the electrostatic attraction toward the latter. Relating to the behavior of the depolarizer, the choice of the supporting electrolyte has to be made on the basis of the following characteristics: it should be chemically not reactive, do not interfere with diffusion and with the electrons exchange on the electrode surface, have a different discharge potential (at least 100 – 200 mV), have high ionic conductivity, and low electrical resistance [41].

### 2.8.6 The Potentiostat

The task of applying a known potential and monitoring the current falls to the potentiostat. A potentiostat will accurately control the potential of the Counter Electrode (CE) against the Working Electrode (WE) so that the potential difference between the working electrode (WE) and the Reference Electrode (RE) is well defined, and correspond to the value specified by the user. In

potentiometric sensors, the potential difference between the reference electrode and the indicator electrode is measured without polarizing the electrochemical cell, that is, very small current is allowed. The reference electrode is required to provide a constant half-cell potential. The indicator electrode develops a variable potential depending on the activity or concentration of a specific analyte in solution. Figure 23 below shows the circuit diagram for potentiostat [35].

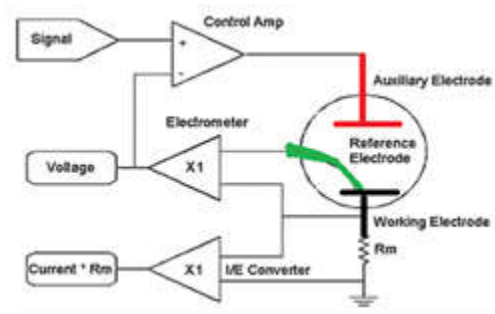


Figure 23: The circuit for potentiostat [35]

### 3 Experimental

#### 3.1 Reagents and Chemicals

All chemicals used were analytical grade and were used without any further purification: catechol  $C_6H_6O_2$ , (research–lab. chem. industries Mumbai (Indian)), 2 mg/mL dispersed in water, graphene oxide (GO) from SIGMA ALDRICH, Bromocresol purple (BCP) 5,5-dibromo-*o*-cresolsulfo phthalein  $C_{21}H_{16}Br_2O_2S$ , monomer, acetic acid,  $CH_3COOH$ , dichloro-phenol,  $C_6H_4OHCl_2$  hydroquinone,  $C_6H_6O_2$ , potassium ferrichexacyanide,  $K_3Fe(CN)_6$ , aluminum oxide,  $Al_2O_3$  a 0.05  $\mu m$  were from. SIGMA ALDRICH, Sodium acetate (anhydrous),  $NaCH_3COO$ , from (BDH), dipotassium hydrogen phosphate,  $K_2HPO_4$  orthophosphate, from (PARK)-scientific-limited Northampton), potassium dihydrogen phosphate,  $KH_2PO_4$ , Hopkin and Williams LTD were from England. Phenol  $C_6H_5OH$  and KCl were from Riedel-de Haën-France.

#### 3.2 Apparatus and Instrumentation

##### 3.2.1 Apparatus

The electrochemical cell consisted of a bare glassy carbon working or poly BCP/ERGO/GCE modified electrodes, Ag/AgCl 3M KCl reference electrode, platinum counter electrode, The cyclic

---

voltammetry apparatus used was CV-50W electrochemical analyzer [Bio-analytical systems (BAS), USA], coupled to a Dell computer (Pentium 4). Voltammetric analyzers CH instruments, (model CHI 760D) and Campar potentiostat, AOC computer, ultrasonic cleaner power-80W, frequency 4 kHz capacity 2 L input-240 VAc 50 Hz, labopette, single channel with 0.5-10  $\mu$ L, 2-20  $\mu$ L, and 100-1000  $\mu$ L volume configuration, certified conformity with tip injection and calibration options (variable volume single channel manual pipettes), pH meter (senses ion TM+MM150) electronic Balance (Model: Scientech: ZSA 120) were also used.

### 3.2.2 Instrumentation

The voltammetric experiments were performed using CV 50W and CHI 760D voltammetric analyzer, a Campar potentiostat, and AOC computer. A conventional three-electrode electrochemical cell was used for the measurements with a bare glassy carbon electrode (GCE), poly BCP/GCE, ERGO/GCE, and poly BCP/ERGO/GCE as the working electrodes, with Ag/AgCl (3 M KCl) at reference, and a platinum wire as counter electrodes. Figure 24 below illustrates the instrumentation of the electrochemical cell for voltammetric determination.

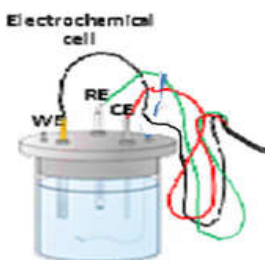


Figure 24: The electrochemical cell for voltammetric determination

## 3.3 Experimental Procedure

### 3.3.1 Preparation of Supporting Electrolytes

The supporting electrolyte of acetate buffer ( $\text{CH}_3\text{COOH}/\text{NaCH}_3\text{COO}$  solution) in the pH range 3-8 was prepared from 0.1 M  $\text{CH}_3\text{COOH}$  and 0.1 M  $\text{NaCH}_3\text{COO}$  in distilled water. The pH of the solutions was calculated by using the Henderson–Hasselbalch equation proportion, and adjusted using pH meter.

---

Phosphate buffer ( $\text{KH}_2\text{PO}_4$  /  $\text{K}_2\text{HPO}_4$ ) of pH 6 used as the background (supporting) electrolyte in electrolytic reduction of GO; and in the electropolymerization of monomer BCP. Phosphate buffer was prepared from 0.1 M  $\text{KH}_2\text{PO}_4$  and 0.1 M  $\text{K}_2\text{HPO}_4$  in distilled water and the pH was adjusted using pH meter.

### **3.3.2 Preparation of Analyte and Modifier Solutions**

To avoid slow oxidation of catechol by  $\text{O}_2$  in the pH range 4-7.4 fresh stock solution of  $10^{-3}$  M catechol was prepared in distilled water and diluted to the required concentrations using 0.1 M acetate buffer pH 6.

$5 \times 10^{-2}$  M solution of bromocresol purple was prepared using 0.1 M phosphate buffer of pH 6 and a  $5 \times 10^{-2}$  M  $\text{K}_3\text{Fe}(\text{CN})_6$  in 0.1 M KCl in equimolar proportion was prepared.

### **3.3.3 Preparation of Interference Solutions**

Interferon solutions such as ascorbic acid, hydroquinone, phenol and dichlorophenol of different concentration were prepared when required.

## **3.4 Electrode Modification**

### **3.4.1 Preparation of the Glassy Carbon Electrode for Modification**

Prior to modification, the surface of the glassy carbon electrode was polished successively with  $0.05 \mu\text{m}$  alumina slurry on polishing kit which is in a lapping cloth to obtain a mirror finished, and cleaned with distilled water. It was also sonicated in methanol and water respectively when required, then allowed to dry in air at room temperature.

### **3.4.2 Modification of the glassy carbon electrode with ERGO**

2.0 mg/mL GO aqueous dispersion was sonicated for an hour in the ultrasonic cleaner. To the clean GCE using,  $3 \mu\text{l}$  the GO solution was carefully put on the top of GCE, and allowed to dry at room temperature to form GO/GCE film. Electrochemical reduction of GO was carried out using the CV-50W or CHI 760D voltammetric analyzers, and a 0.1 M phosphate buffer ( $\text{KH}_2\text{PO}_4$ /  $\text{K}_2\text{HPO}_4$ ) solution of pH 6 as supporting electrolyte in the potential range -1.2 to 2.0 V versus Ag/AgCl/saturated KCl (3 M KCl) at scan rate of 100 mV/s for 15 cycles as illustrated in Figure 25. The

---

electrochemical reduction of GO was optimized by 15 cycles. The electrochemically reduced graphene oxide on glassy carbon electrode (ERGO/GCE) was rinsed using distilled water to remove physically adsorbed and un-reacted GO, and allowed to dry in air.

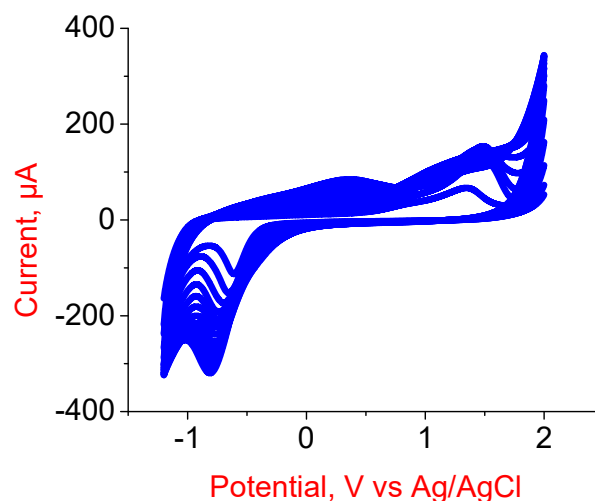


Figure 25: Cyclic voltammogram of the electrochemical reduction of GO film on glassy carbon electrode in phosphate buffer solution at a pH 6 in the potential range -1.2 V to 2.0 V vs Ag/AgCl/(3 M KCl) at scan rate of 100 mV/s for 15 cycles

### 3.4.3 Modification of ERGO/GC Electrode with poly BCP

The electropolymerization of BCP on the electrochemically reduced graphene oxide modified electrode (ERGO/GCE) was carried out using the  $5 \times 10^{-2}$  M bromocresol purple monomer in 0.1 M phosphate buffer (pH 6) as supporting electrolyte in the potential range of -0.10 V to 1.60 V versus Ag/AgCl at a scan rate of 100 mV/s for 15 cycles. The cyclic voltammogram of the polymerization is illustrated in figure 26. The poly BCP/ERGO/GCE; modified electrode was rinsed using distilled water to remove physically adsorbed and unreacted BCP and allowed to dry in air. Electropolymerization of the poly BCP was optimized at the electrochemically reduced graphene oxide (ERGO) with 3  $\mu$ L of 2 mg/mL GO film on GCE in 0.05 mM BCP in PBS (pH 6) for 15 cycles. Finally, the modified electrode was dried in air and made ready for use.

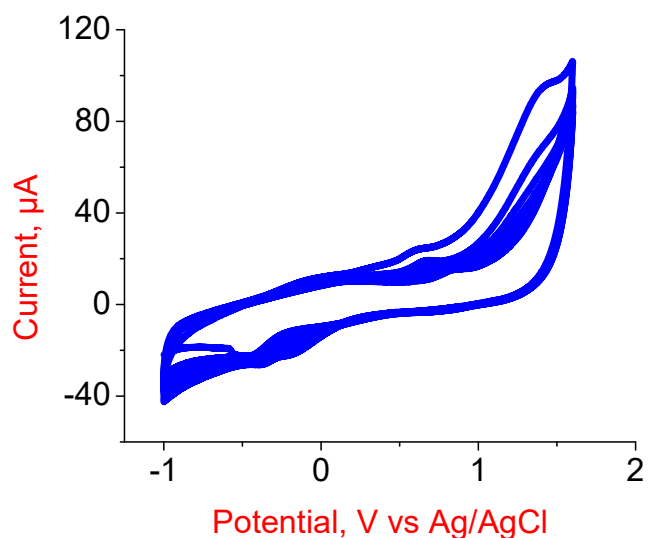


Figure 26: Cyclic voltammogram for the electropolymerization of  $5 \times 10^{-2}$  M bromocresol purple monomer in a 0.1 M phosphate buffer (pH-6) in the potential range of -0.10 V-1.60 V versus Ag/AgCl (3 M KCl) at a scan rate of 100 mV/s for 15 cycles on electrochemical reduced GO modified electrode (ERGO/GCE)

## 4 Results and Discussion

### 4.1 Comparison of Bare, poly BCP/GCE, ERGO/GCE and poly BCP/ERGO/GCE

From Figure 27 (a) it can be seen that at the bare electrode, the oxidation and reduction of catechol result in broad waves with the corresponding peak potentials of 408 mV and 127 mV. Hence it shows irreversible behavior at the bare GC, and very low electrocatalytic activity. At the poly BCP/GCE (Figure 27 (b)), the reversibility of catechol is improved together with increasing current signal. The oxidation peak potential negatively shifts to 333 mV and the reduction peak positively shifts to 259 V with ( $\Delta E_p = 74$  mV). In addition, at the ERGO/GCE modified electrode (Figure. 27 (c)) the reversibility of catechol is improved. The oxidation peak potential negatively shifts to 294 mV and the reduction peak positively shifts to 238 V with ( $\Delta E_p = 56$  V). But at the composite poly BCP/ERGO/GC modified electrode (Figure 27. (d)) the oxidation peak potential negatively shifts to 288 mV and the reduction peak positively shifts to 223 mV with ( $\Delta E_p = 63$  mV) where, the reversibility of catechol is significantly improved.

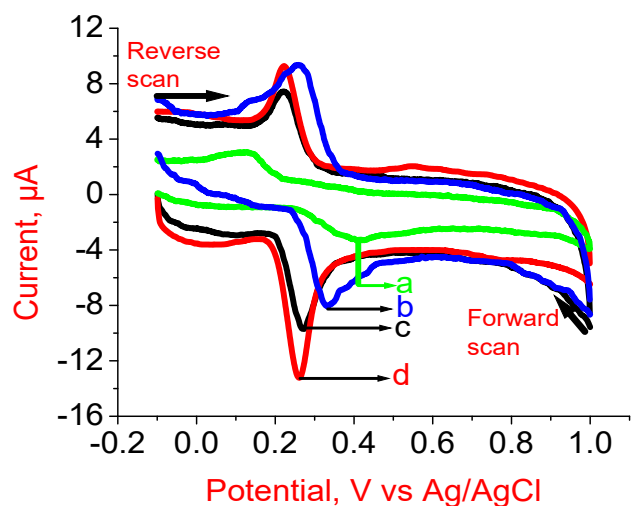


Figure 27: Cyclic voltammogram of 100  $\mu\text{M}$  catechol at different electrodes (a) bare GCE (b) poly BCP/GCE c) ERGO/GCE, and d) poly BCP/ERG/GCE at scan rate of  $100 \text{ mVs}^{-1}$  in 0.1 M ABS solution pH 6.0.

## 4.2 Electrochemical Responses for CC at poly BCP/ERGO/GCE

In order to investigate the oxidation and reduction behavior of catechol at the poly BCP/ERGO/GC modified electrode the obtained result was compared with theoretical value. In CV for a reversible electrode reaction the Ratio of  $i_{pa} / i_{pc}$  and the difference in peak potential for two electron transfer is one and 29 mV respectively. As shown in Table 4 the experimental value of the poly BCP/ERG/GC modified electrode 1.06 and 31.5 mV is satisfactory in comparison with the theoretical values.

Table 4 Electrochemical Response Measurement at poly BCP/ERGO/GCE

Types of Electrode	$E_{pa}$ , (mV)	$E_{pc}$ , (mV)	Change in $E_p$ , ( $\Delta E_p$ ) mV	$i_{pa}$ , ( $\mu A$ )	$i_{pc}$ , ( $\mu A$ )	$i_{pa} / i_{pc}$
Bare/GCE	408	127	281	2.368	-1.811	1.31
Poly/BCP/GCE	333	259	74	8.235	-6.818	1.2
ERGO/GCE	294	238	56	10.941	-8.754	1.25
Poly BCP/ERGO/GCE	288	223	65	13.011	-12.321	1.06

5 mM  $K_3Fe(CN)_6$  in 0.1 M KCl (equimolar) was also used as a probe to measure the effective surface area of the poly BCP/ERGO/GC modified electrode and bare GCE using cyclic voltammetry (Figure 28). Based on the voltammogram obtained the effective surface area was calculated using, the peak current  $i_p$  for a reversible system as described by the Randles Sevcik equation;

$$i_p = (2.69 \times 10^5) n^{3/2} A D^{1/2} \nu^{1/2} C$$

for the forward reaction:  $[Fe(CN)_6]^{-3} + e^- \rightleftharpoons [Fe(CN)_6]^{-4}$

Where  $i_p$  is current in  $A$ ,  $n$  number of electrons in the redox reaction,  $A$  is the electrode surface area in  $cm^2$ ,  $D$  (in  $Cm^2/s$ ) is the diffusion coefficient for the reduction (forward sweep)  $C$  the concentration  $mol/cm^3$ , and  $\nu$  the scan rate  $Vs^{-1}$ . The calculated electrochemical active surface area of the bare GCE was  $0.039 cm^2$  and that of poly BCP/ERGO/ GC modified electrode was  $0.056 cm^2$ .

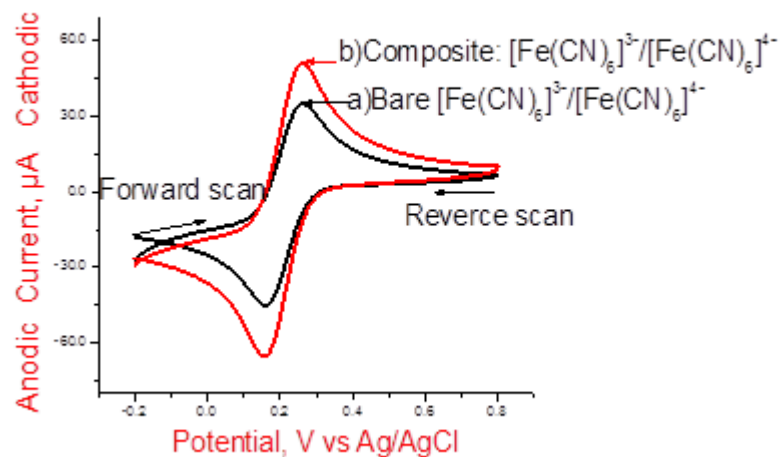


Figure 28: Cyclic voltammetric signals of  $5 \times 10^{-2}$  M  $[\text{Fe}(\text{CN})_6]^{3-}/[\text{Fe}(\text{CN})_6]^{4-}$  in 0.1 M KCl (equimolar) at a scan rate of 100 mV/s: a) Bare GCE b) poly BCP/ERGO/GCE

### 4.3 Cyclic voltammetric Analyses of Catechol

The cyclic voltammogram of catechol shows reversible oxidation and reduction peaks. The cyclic voltammogram for the electrochemical reaction of catechol at poly BCP/ERGO/GC modified electrode for  $10^{-4}$  M CC at pH 6 ABS and scan rate of 100 mV/s is shown in Figure 29. It showed an oxidation peak at 288 mV and a reduction peak at 223 mV. The separation of peak potentials was about 63mV with ratio of  $i_{pa} / i_{pc}$  of 1.06.

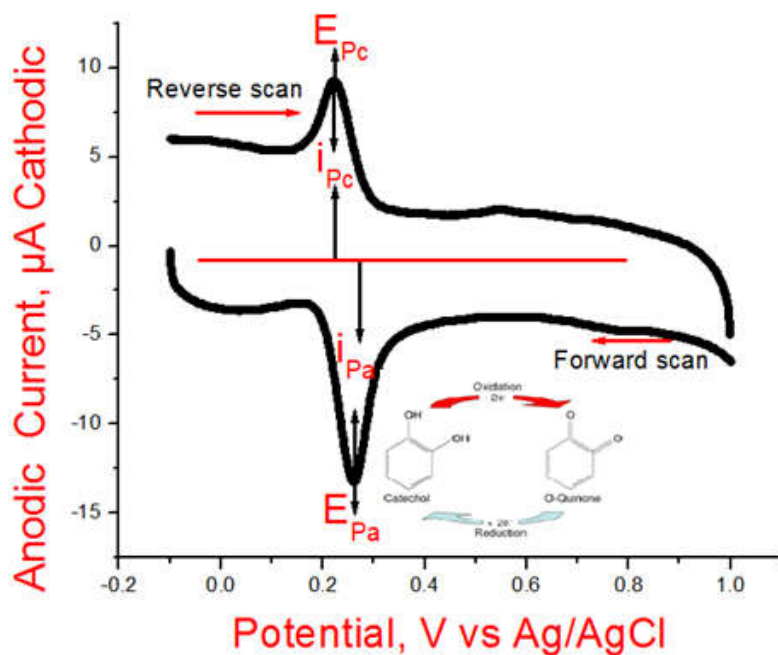


Figure 29: Cyclic voltammogram of 0.1 mM CC in pH 6 ABS and scan rate of 100 mV/s

The anodic and cathodic reactions of CC as seen in Figure 30 takes place at the surface of the poly BCP/ERGO/GC modified electrode as suggested by the following reaction scheme

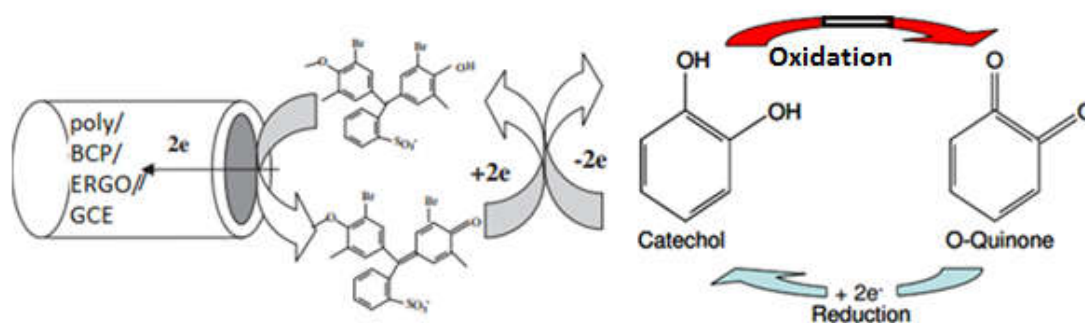


Figure 30 Electrocatalytic oxidation reaction of CC at the poly BCP/ERGO/GC modified electrode

### 4.3.1 Effect of scan rate

The oxidative current of  $10^{-4}$  M catechol at the poly BCP/ERGO/GC modified electrode in a 0.1 M acetate buffer pH 6 electrolyte solutions was studied. Figure 31 shows the cyclic voltammogram obtained in the potential range of 0.0- 0.5 V. To investigate the diffusion behavior CVs were recorded for the scan rate range 25 – 600 mV/s and a shift in the anodic peak potentials, and change in the magnitude of the anodic peak currents were observed. Hence it was found that the electrode reaction of catechol at the surface of poly BCP/ERGO/GC modified electrode depends on the scan rate.

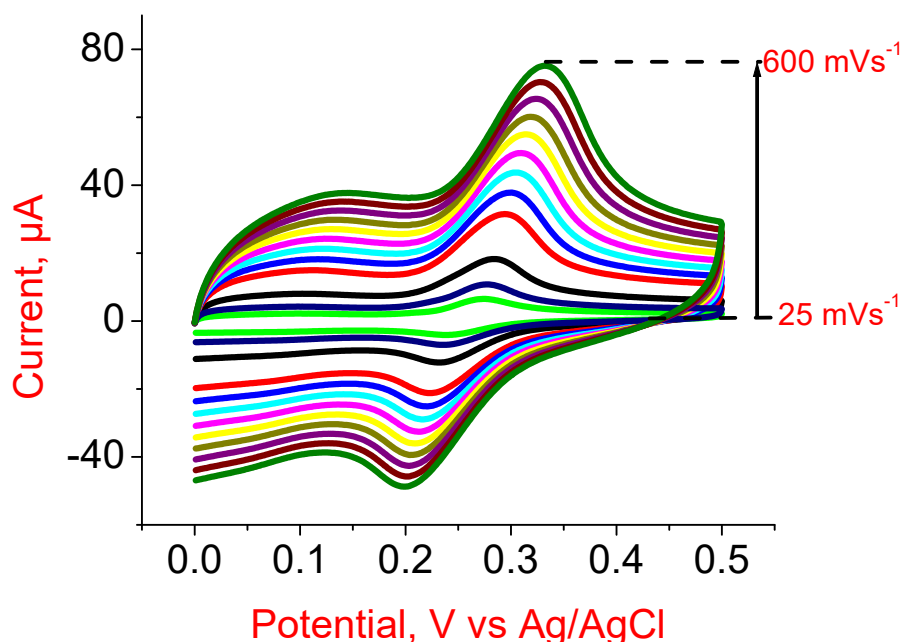


Figure 31: Cyclic voltammogram recorded at poly BCP/ERGO/GCE for  $10^{-4}$  M CC in 0.1 M acetate buffer solution (pH 6.0) at different scan rates (mV/s) 25, 50, 100, 150, 200, 250, 300, 350, 400, 450, 500, 550, and 600.

In order to investigate the effect of scan rate on the oxidative and reductive peak currents of  $10^{-4}$  M catechol at poly BCP/ERGO/GCE in 0.1 M acetate buffer solution (pH = 6) were analyzed. Figure 33 shows both the oxidative and reductive peak current of catechol increased with increased scan rate (100 - 450 mV/s). Figure 32 also show that the oxidation and the reduction peak currents of catechol exhibited a linear relationship with the square root of the scan rate in the range 100 to

450 mV/s. The linear regression coefficient of the  $I_{pa}$  and  $I_{pc}$  verses square roots of the scan rates are 0.999 and 0.999 respectively which is almost one. The relationship between the oxidation peak current and square root of the scan rate indicates that the oxidation of CC at the composite modified electrode is a diffusion-controlled process.

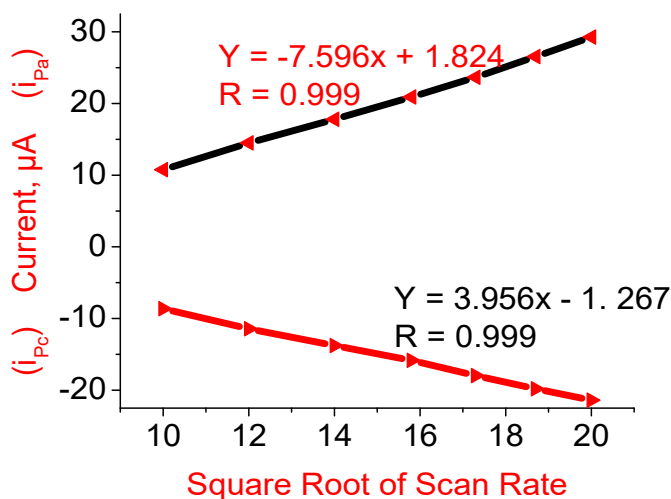


Figure 32: The dependence of the anodic and cathodic peak currents on square root of scan rate

It can also be seen that with increasing scan rate, the peak potentials shifted as shown in Figure 33. The anodic peak potential shifted to more positive potential values, while that of the cathodic peak shifted to more negative value

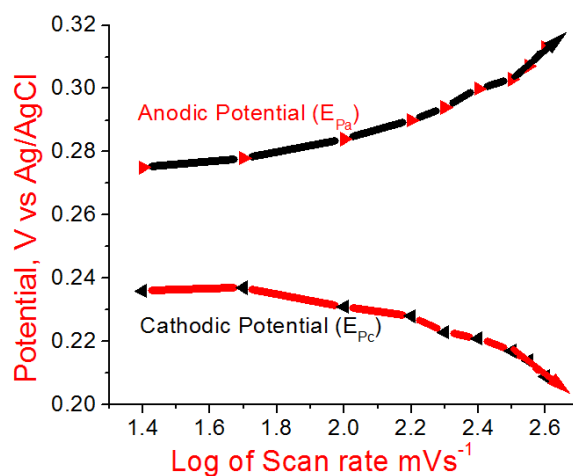


Figure 33: The dependence of the anodic and cathodic peak potential ( $E_p$ ) on log of scan rate  $mVs^{-1}$

### 4.3.2 Effect of pH of the supporting electrolyte

The pH of the media (supporting electrolyte) used has a profound effect on the voltammetric response. It affects the rate, equilibrium state and the electrode reaction. For this reason the parameter was studied using CV as illustrated in Figure 34 for catechol determination at the poly BCP/ERGO/GC modified electrode in the pH range 3 to 8. Shift of peak potentials towards less positive potential indicates the modified electrode acts as a good electrocatalyst.

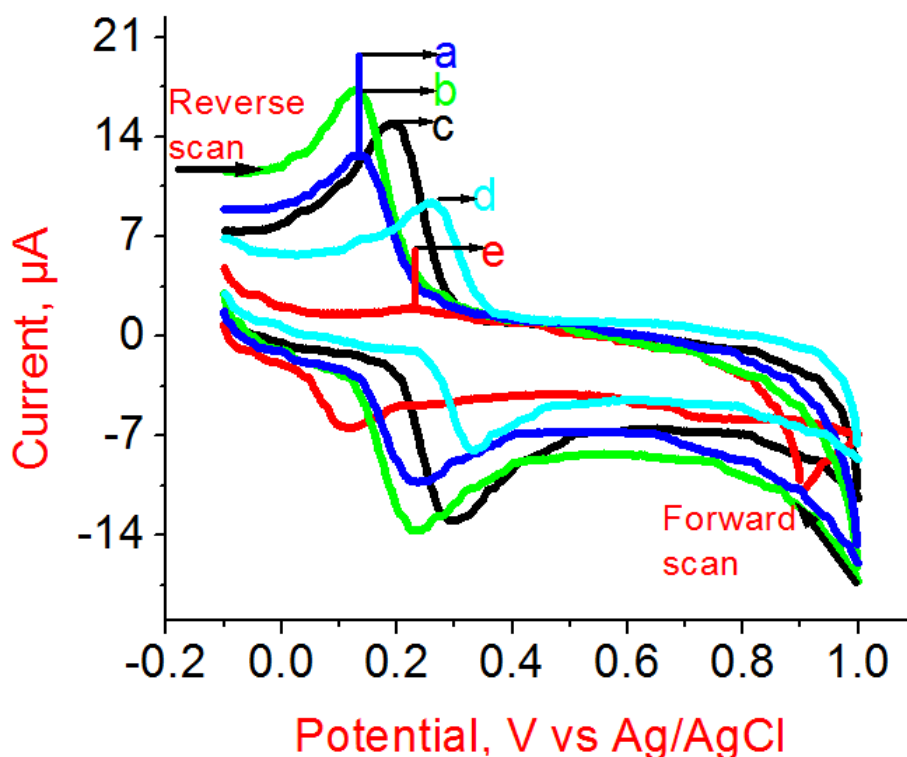


Figure 34: The effects of pH on the response for  $10^{-4} M$  catechol in 0.1 M acetate buffer solution at poly BCP/ ERGO/GCE at scan rate of  $100 \text{ mVs}^{-1}$  a) pH 5 b) pH 6 c) pH 7 d) pH 7.5 e) pH 8.

The peak current of catechol as a function of pH is shown in Figure 35. Catechol shows different voltammetric behavior in the pH range studied; this may be due to the influence of pH of supporting electrolyte on the accumulation potential. According to the observed results the amount of accumulated catechol at poly BCP/ERGO/GC modified electrode is largest at pH 6.0. Figure 35 also shows that the anodic peak current increased as the pH increased and reaches the highest peak at (pH 6) and then decreases. The optimum pH needed to study the electrochemical reaction of catechol at the poly BCP/ ERGO/GC modified electrode was determined to be pH 6.

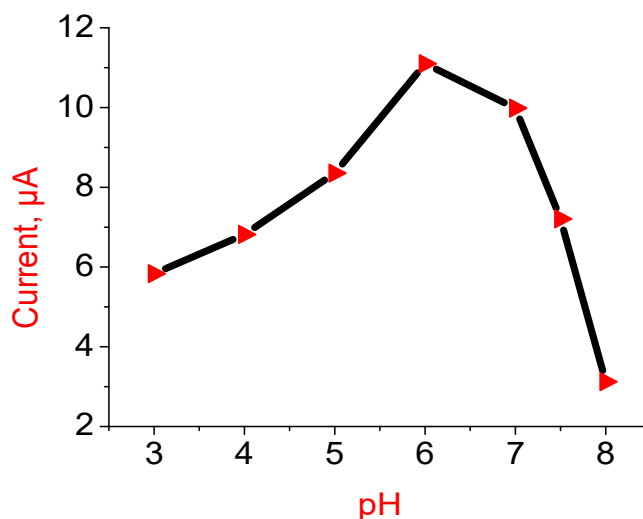


Figure 35 Plot of anodic peak currents as a function of pH for  $10^{-4}$  M catechol at  $100 \text{ mVs}^{-1}$

#### 4.4 Differential pulse voltammetric analysis

##### 4.4.1 Optimization of DPV Experimental Parameters

The effect of the parameters for differential pulse voltammetric determination of catechol at poly BCP/ERGO/GC modified electrode was optimized as presented in Table 5. Optimum conditions for the electrochemical response were established by measuring the peak current on dependence on all parameters increment, amplitude, pulse width, sample width, pulse period, and quiet time. The optimum parameters identified for the determination of the analyte for plotting the calibration curve are summarized in Table 5.

Table 5 Parameters and Optimum Values of DPV Experimental Conditions

Parameter	Optimization range	Optimum Value
Increment	0.001-0.006	0.003
Amplitude (V)	0.03-0.1	0.06
Pulse width (sec)	0.02-0.07	0.05
Sample width(sec)	0.015-0.018	0.0175
Pulse period (sec)	0.1- 0.4	0.2
Quiet time (sec)	-	2
Sensitivity (A/V)	$10^{-6}$ - $10^{-4}$	$10^{-4}$
pH	3-8	6

#### 4.4.2 Linear Range and Detection Limit

The analytical usefulness of a given experiment depends on achieving well defined concentration dependence. According to the optimum experimental conditions described above; the dependency of the voltammetric signal on the concentration of catechol and the sensitivity of the method are illustrated by differential pulse voltammetry for different concentration of catechol. Figure 36 shows some of the typical DPV voltammograms recorded at the poly BCP/ERGO/GC modified electrode for different catechol concentrations.

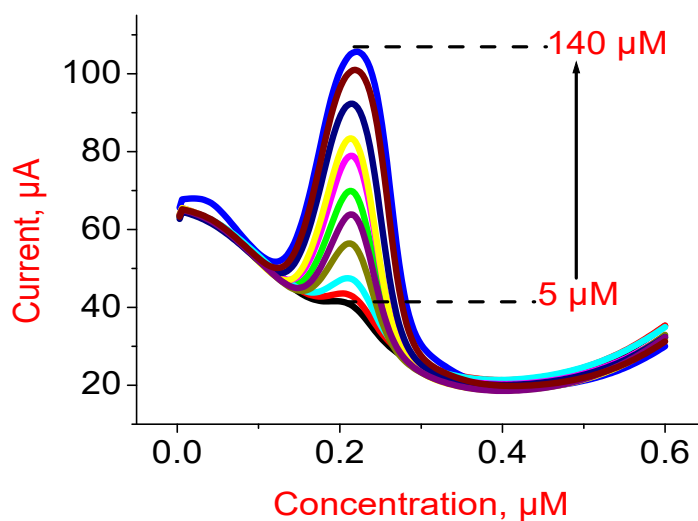
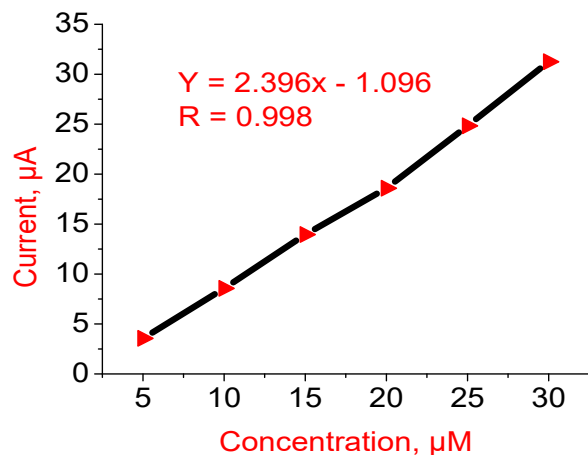


Figure 36: Differential pulse voltammograms at poly BCP/ERGO/GC modified electrode for different concentrations of catechol

The peak height for catechol was found to increase with an increase in concentration from 5.0 to 140 µM. The calibration curves for data points was found to be linear with  $R = 0.998$ , the numerical value of regression coefficient,  $R$  for this experiment, the data sets showed a good linear fit because the value of  $R$  is almost one. The detection limit for catechol, at this electrode was found to be 0.5 µM. Figure 37 shows the calibration curve for the differential pulse voltammetric responses for catechol at poly BCP/ERGO/GC modified electrode in the concentration range 5-30 µM.



---

Figure 37: Plot of DPV anodic peak current as a function of catechol concentration from 5-30  $\mu\text{M}$

#### 4.4.3 Comparison with Reported works

Voltammetric determinations of catechol at different modified electrodes have been reported. Table 6 shows performance comparison of poly BCP/ERGO/GCE with other composite modified electrodes for catechol detection using voltammetric techniques. From the comparison of the present work with the already reported works it can be inferred that the present work is comparable or satisfactory.

Table 6: Comparison of Characteristics Values Obtained from Some Literatures and This Work.

Sensors	Linear Range ( $\mu\text{M}$ )	LOD ( $\mu\text{M}$ )	Reference
SWCNT/PEDOT/GCE	6-100	0.18	[9]
Screen Printed Graphite Electrode	1-100	0.29	[10]
CPE modified with Anthraquinone	6-80	0.2155	[13]
Penicillamine/GCE	25-175	0.6	[14]
Tyr/GCE	60-80	6	[15]
CILE/GCE	1-800	0.6	[16]
MWCNTs/GCE	20-120	10	[17]
p-Phe/GCE	10-140	0.7	[18]
Poly BCP/ERGO/GCE	5-140	0.8	This work

#### 4.4.4 Effect of Interferences

Possible interferents in the detection of catechol such as ascorbic acid, hydroquinone, phenol and dichlorophenol at poly BCP/ERGO/GC modified electrode were studied. Different  $\mu\text{M}$  of the interferon were added to constant concentration (20  $\mu\text{M}$ ) of catechol and differential pulse voltammograms were recorded between 0.01 V and 1.0 V.

## 1) The effect of Ascorbic acid

Figure 38 shows the effect of the addition of 20, 60, and 100  $\mu\text{M}$  ascorbic acid (AA) added to 20  $\mu\text{M}$  CC. The voltammograms indicate the peak current of AA has no marked effect on the response of catechol though there is a negligible decrease in the peak currents of catechol as the concentration of ascorbic acid increases. Showing that catechol can be detected in the presence of ascorbic acid at the poly BCP/ERGO/GC modified electrode.

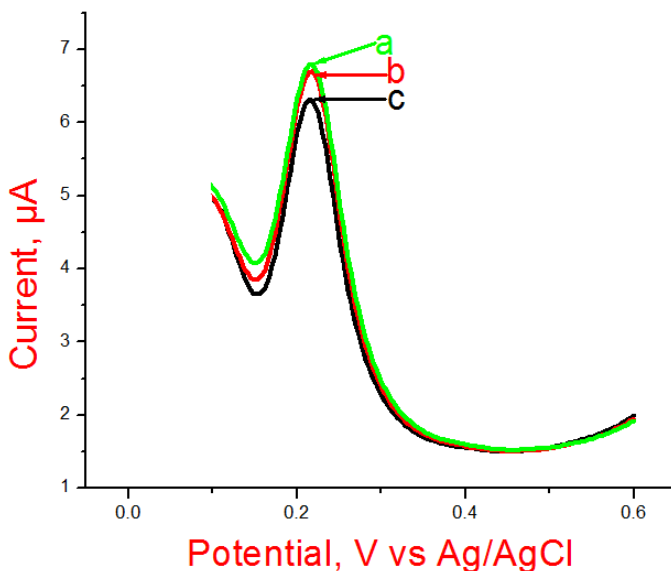


Figure 38 Differential pulse voltammograms at poly BCP/ERGO/GC modified electrode for 20  $\mu\text{M}$  CC and a) 20 b) 60 and c) 100  $\mu\text{M}$  ascorbic acid (AA)

## 2) The effect of Hydroquinone

The Interference study or hydroquinone was performed using DPV at poly BCP/ERGO/GC modified electrode for 20, 100, and 200  $\mu\text{M}$  hydroquinone spiked to 20  $\mu\text{M}$  catechol. Figure 39 shows a linear increase in the response for hydroquinone and did not affect the response current of catechol, with a negligible decrease the peak current for catechol remained constant and overlapping peaks of catechol with no shift were observed. The DPV voltammograms showed hydroquinone and catechol can be simultaneously determined by using this composite modified Electrode.

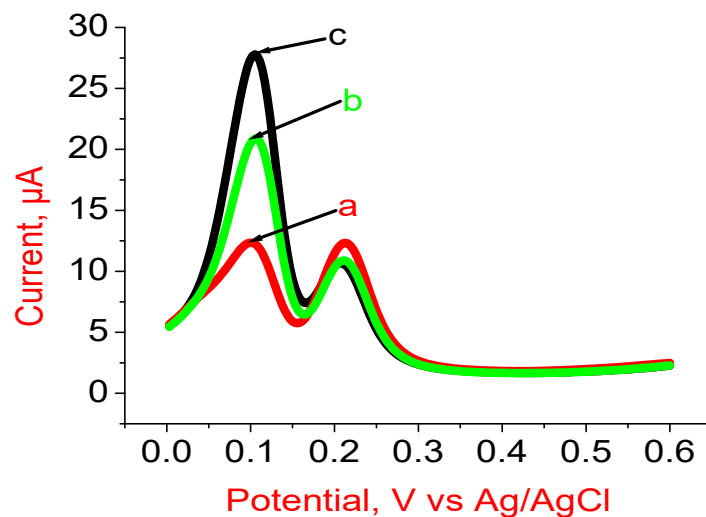


Figure 39 Differential pulse voltammograms at poly BCP/ERGO)/GC modified electrode in a 0.1 M ABS (pH-6) for a) 20 b) 100 and c) 200  $\mu\text{M}$  hydroquinone (HC) spiked to 20  $\mu\text{M}$  CC

### 3) The effect of Phenol

Phenol which is the most environmental interfering organic compounds was examined as interferon to CC. To examine this a) 20 b) 60 c) 80 and d) 200  $\mu\text{M}$  of phenol were spiked to 20  $\mu\text{M}$  CC. As shown in Figure 40 the oxidation peak current for phenol increased proportionally to the concentrations from 20 to 60  $\mu\text{M}$ . At this concentration (60  $\mu\text{M}$ ), unexpected increase in peak current of CC was also observed, and it is also clearly seen that the rapid fall of the peak current of phenol and CC in the concentrations 80 and 200  $\mu\text{M}$  at this composite modified electrode indicates the redox behavior of phenol at the electrodes. These effects can be attributed to the series of phenolic redox reactions as illustrated in Figure 41.

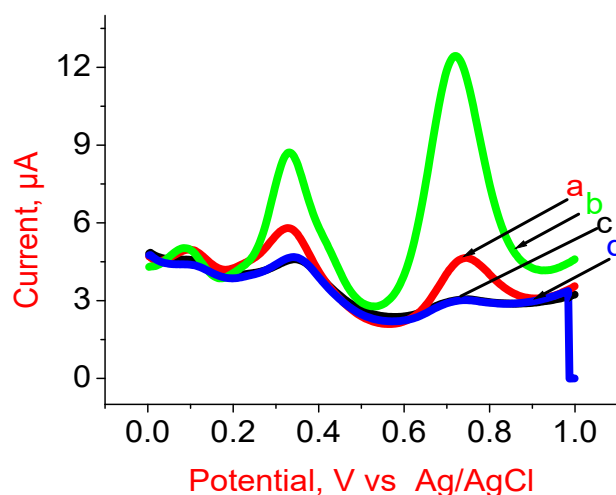


Figure 40 Differential pulse voltammograms at poly BCP/ERGO/GC modified electrode in a 0.1 ABS (pH-6) for a) 20 b) 60 c) 100 and d) 200  $\mu\text{M}$  phenol spiked to 20  $\mu\text{M}$  CC

The increase in the peak current of CC is due to the additional CC formed in the redox reaction of phenol at the electrode. The peak currents on the left at more negative potential is that of HQ as it is one of the products of phenol redox reaction at the electrode. The decrease in the peak currents of the compounds when the concentration of phenol is increased can be due to the electro-inactive product (figure 41) causing fouling of the electrode.

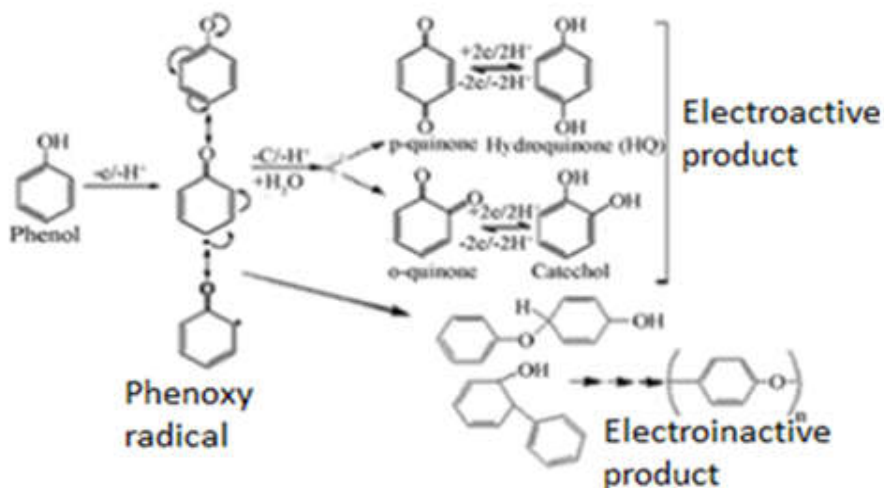


Figure 41 Possible redox reactions of phenol at the electrode

#### 4) The effect of Dichlorophenol

Dichlorophenol with higher oxidation potential than CC is examined to see its interference in CC determination. To examine this a) 20 b) 40 and c) 60  $\mu\text{M}$  of dichlorophenol were spiked to 20  $\mu\text{M}$  catechol. As can be seen from the voltammograms in Figure 42, dichlorophenol does not interfere in the responses for catechol, the peak current of catechol remained constant and overlapping peaks of catechol with no shift were observed. Showing that catechol can be detected in the presence of dichlorophenol at this modified electrode.

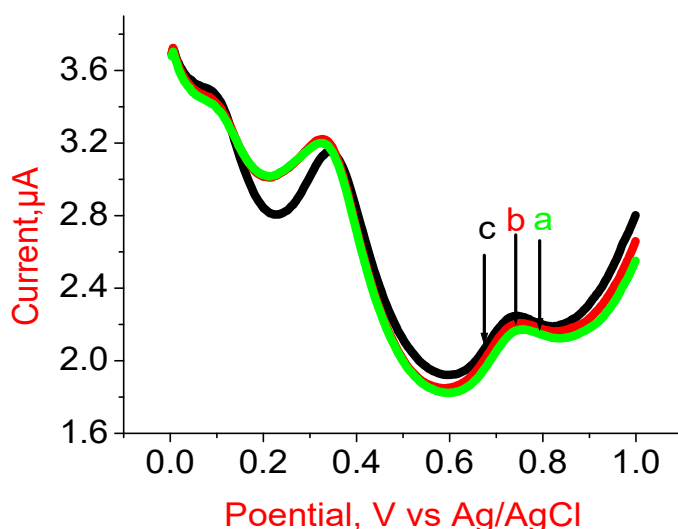


Figure 42 Differential pulse voltammogram at poly BCP/ERGO/GC modified electrode in a 0.1 ABS (pH-6) for a) 20 b) 40 and c) 60  $\mu\text{M}$  dichlorophenol spiked to 20  $\mu\text{M}$  CC

#### 4.4.5 Determination of CC in Tap water

To verify the analytical applicability of the sensor, the CC in tap water sample was determined by the poly BCP/ERGO/GC modified electrode. DPV method was used to detect CC in the tap water. In the absence of CC for 4 mL water (real) sample and 6 mL ABS (0.1M, pH-6), peak current was not observed. However the modified electrode gave correspondingly higher peak currents for increasing concentration of CC spiked to the pH 6 ABS and fixed amount of tap water sample as shown in figure 43, which shows that CC was absent in the tap water sample.

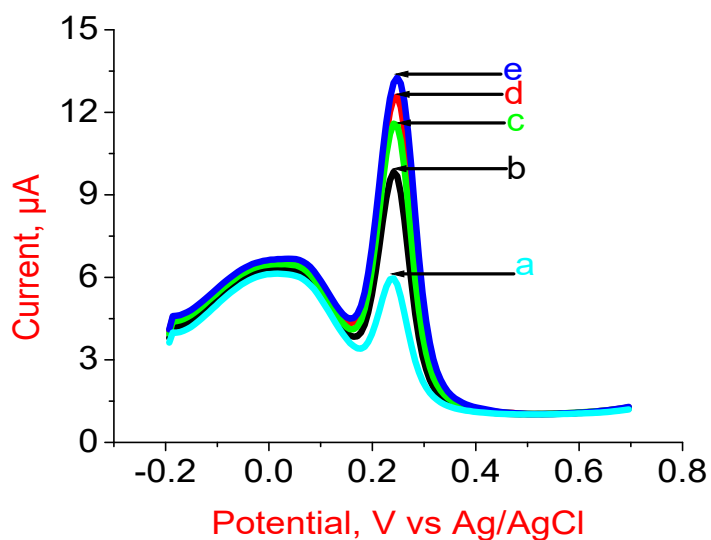


Figure 43 Differential pulse voltammograms at poly BCP/ERGO/GC modified electrode in 0.1 M ABS (pH-6) for a) 500 b)1000 c)1500 d) 2000 and e) 2500  $\mu\text{L}$  of  $10^{-4}$  M spiked to 6 mL ABS and 4 mL of tap water.

Known concentration of CC containing tap water samples were spiked into the pH 6 ABS solution. The recovery values were calculated in terms of current produced for pure CC and Spiked CC in the tap water samples as summarized in Table 7 assuming that current is directly proportional to concentration.

Table 7 Recovery Study

Tap water in ABS	$10^{-4}$ CC ( $\mu\text{L}$ )	Current ( $\mu\text{A}$ ) Pure CC	Current ( $\mu\text{A}$ ) Spiked CC	Recover %
4 mL in 6 mL	500	6.115	5.893	103.7
4 mL in 6 mL	1000	10.052	9.952	100.1
4 mL in 6 mL	1500	11.613	11.726	98.7
4 mL in 6 mL	2000	11.883	12.263	96.9
4 mL in 6 mL	2500	12.575	13.14	95.7

---

## 5 Conclusions

In this work, a novel poly bromocresol purple was prepared by simple and fast electropolymerization method; on a film of electrochemically reduced graphene oxide on glassy carbon electrode (poly BCP/ERGO/GC modified electrode). The modified electrode was characterized and used as an electrochemical sensor for the determination of CC by CV and DPV respectively. The modified electrode had good sensitivity and selectivity. The results demonstrated that the proposed method is rapid, sensitive, and reproducible for the determination of catechol. Hence, the poly BCP/ERGO/GC modified electrode can be a useful tool for the assay of CC both in research and in detection of CC in real sample (water, medicines etc.) even in the presence of expected interferon compounds such as hydroquinone, ascorbic acid phenol etc. Since the BCP/ERGO/GC modified electrode showed satisfactory result for the direct determination of CC by differential pulse voltammetry (DPV), it can also be used in several sensor applications for environmental and biological molecules of interest.

---

## 6 References

1. A. C. Morrin, Electroanalytical Sensor Technology. National Centre of Sensor Research, School of Chemical Sciences (2013), Vol: 10, pp 5772/51480
2. N. Sedhu, V. Raj, 1,2 Advanced Materials Research Lab Department of Chemistry, Periyar University, IRJET (2017), Vol: 04(09), pp 636 011
3. L. A. Alshahrani, Xi Li , H. Luo, L. Yang, M. Wang, S.Yan, P.Liu, Y. Yang and Q. Li, Sensors (2014), Vol: 14, pp 22274-22284
4. H.L. Guo, X.F. Wang, Q.Y. Qian, F.B. Wang, X.H. XiaA green approach to the synthesis of graphene nanosheets, ACS Nano (2009), Vol:3, pp 2653–2659.
5. M. Sittig. Handbook of Toxic and Hazardous Chemicals and Carcinogens. 2nd ed. Noyes Publications, Park Ridge, NJ. IARC MONOGRAPHS (1987), Vol: 71 pp 433-435
6. A. B. Teradale, S. D. Lamani, B. E. Kumara Swamy, P. S. Ganesh, and S. N. Das, Electrochemical Investigation of Catechol at Poly(niacin amide) Modified Carbon Paste Electrode; Advances in Physical Chemistry A Voltammetric Study Hindawi Publishing Corporation Volume (2016), Article ID 8092860, 8 pages
7. N. Schweigert, J. B. Alexander Zehnder and I. L Rik. Eggen, Environmental Microbiology (2001), Vol: 3(2), pp 81-91
8. P. H. Dykstra An Optical MemS Sensors For Chip catechol Detection (2008), pp 9-10
9. T.G/hiwot, M. Tessema, Electrochemical Determination of Catechol using SWCNT/PEDO T/GC modified electrode (2014), Addis Ababa University School of Graduate Studies
10. G. A. M. Mersal, Electrochemical Sensor for Voltammetric Determination of Catechol Based on Screen Printed Graphite Electrode Chemistry Department (2009), Int. J. Electrochemical. Sci., (2009) Vol: 4, pp 1167 - 1177
11. T. Kasa, T. Solomon, Cyclic Voltammetric and Electrochemical Simulation Studies on the Electro-Oxidation of Catechol in the Presence of 4, 4- bipyridine. AJPC (2016), Vol: 5(3), pp. 45-55.
12. J. Q. Y. Wang, Y.Dong, Z. Zhu and H. Xing, Sensitive determination of catechol using a glassy carbon electrode modified with L-cysteine and ZnS:Ni/ZnS quantum dots RSC Advanced (2015), Vol: 7, pp 260-265

- 
13. F. Melak, M. Redi , M. Tessema , and E. Alemayehu. Electrochemical Determination of Catechol in Tea samples Using Anthraquinone Modified Carbon Paste Electrode. *Natural Science* 58107 (2013), Vol: 5(8), pp 888-894
  14. L. Wang, P.F. Huang, J.Y. Bai, H.J. Wang, L.Y. Zhang and Y.Q. Zhao, Covalent Modification of Glassy Carbon Electrode With Aspartic Acid for Simultaneous Determination of Hydroquinone and Catechol, *Microchim Acta* (2007), Vol: 51 pp 1581.
  15. S. Tembe, S. Inamdar, S. Haram, M. Karve and S.F.D. Souza, Electrochemical material science Biosensors Li-ion battery energy materials, *J. Biotechnol* (2007), Vol: 128 pp 80 - 85.
  16. W. Sun, Y. Li, M. Yang, J. Li and K. Jiao. Application of carbon ionic liquid electrode for the electro oxidative determination of catechol *Sens Actuators B* (2008), Vol: 133 pp 387–392.
  17. Z. Xu, X. Chen, X.H. Qu and S.J. Dong. Carbon Nanotechnology Recent Developments in Chemistry, Physics, Materials, *Electroanalysis* (2004), Vol: 16 pp 684
  18. L. Wang, P. Huang, J. Bai, H. Wang, L. Zhang and Y. Zhao. Simultaneous Electrochemical Determination of Phenol Isomers in Binary Mixtures at a Poly (phenylalanine) Modified Glassy Carbon Electrode, *Int. J. Electrochem. Sci* (2006), Vol: 1 pp 403-413.
  19. A. J. Bard, Murray, R.W, Chemical Modification of Electrodes in "Electroanalytical Chemistry (1983), Vol: 13 pp 135-141
  20. S. Dong and Y. Wang. The Application of Chemically Modified Electrodes in Analytical Chemistry. *Electroanal* (1989) Vol: 1(2), pp 99-106
  21. R. Hoffmann, A. Kabanov, A. Golov, D. Proserpio. Home Citans and Carbon Allotropes. *For an Angwandte Chemie* (2016) Vol: 55 (37), pp 10962 - 10976
  22. The allotropes of carbon, from Wikipedia the free encyclopedia.
  23. J.N Fuchs, M. Oliver. GOERBIG Lecture Notes (2008), Introduction to the Physical Properties of Graphene.
  24. G. Shao, Y. Lu, F. Wu, C. Yang, F. Zeng, Q. Wu. Graphene oxide: the mechanism of oxidation and exfoliation, *J. Mater. Sci.* (2012), Vol: 47 pp 4400.
  25. S. Yong Toh, K. S. Loh, S. K. Kamarudin , W. R.W. Daud, Graphene production via electrochemical reduction of graphene oxide: Synthesis and characterization. *Chem. Eng. J.* (2014), Vol: 251 pp 422–434

- 
26. A. J. Heeger, Semiconducting and metallic polymers: The fourth generation of polymeric materials, *Rev. Mod. Phys* (2001), Vol: 73(3), pp. 681-685
  27. I. György "Chapter 1: Introduction". In Scholz, F. *Conducting Polymers: A New Era in Electrochemistry. Monographs in Electrochemistry. Springer* (2008), Hand books 978-3-540-75929-4 pp 1-6
  28. M. Ates, T. Karazehira, A. S. Sarac *Conducting Polymers and their Applications in Current Physical Chemistry Research Gates* (2012) Vol: 2(3), pp 224 -240
  29. R. E. Barker, JR *Mobility and Conductivity of ions in and into Polymeric solids Pure &Appli. Chem.*, (1976) Vol: 46, pp. 157-170..
  30. H. Shirakawa, E.J. Louis, A.G. MacDiarmid, C.K. Chiang, and A.J. Heeger, *J Chem. Soc. Chem. CROW logo* (2015), *Polymer Properties Database Comm.*, Vol: 72 (5-6), pp 587-587
  31. Ito, Shigenori, Yamamoto, and Daisuke, "Mechanism for the color change in bromocresol purple bound to human serum albumin". *Clin. Chim. Acta.* (2010), Vol: 411 (3): pp. 294–295.
  32. S. Koçak , B.Aslışen , and Ç.C. Koçak *Determination of Hydrazine at a Platinum Nanoparticle and Poly(Bromocresol Purple) Modified carbon nanotube electrode* (2016), Vol: 49(7), pp 990–1003
  33. Y. Wang, L. Tong *Electrochemical sensor for simultaneous determination of uric acid, xanthine and hypoxanthine based on poly (bromocresol purple) modified glassy carbon electrode Sens Actuators B* (2010), Vol:150 pp.43–49
  34. Z., L., *Handbook of Electrochemistry Amsterdam Elsevier* (2007), Vol: 0-444 pp 51958-0A
  35. B. J. Allen, R. Larry, Faulkner, *Electrochemical methods; Fundamentals and Application* (2 ed) , Wiley (2000), Vol: 0-471 pp-04372-9.
  36. Royce. *Analytical chemistry; Electrochemical Pretreatment of Glassy Carbon Electrode C Engstrom* (1982), Vol: 54(13) pp 2310-2314
  37. R.W. Murra, J. B Good enough J.B and W. J Albery *Modified electrodes: Chemically modified electrodes for electrocatalysis. CASSI* (1981), pp 253-265
  38. F. Scholz *Electroanalytical Methods Guide to Experiments and Applications Second, Revised and Extended Edition* (2010), pp 273-333
  39. F.Scholz's *Voltammetric techniques of analysis: the essentials Chem. Texts Springer International Publishing* (2015), Vol: 1 pp 17

- 
40. G. Krishan Cyclic Voltammetry Center for Electrochemical Engineering Research  
Department of Chemical and Biomolecular Engineering (2011), OHIO University.
41. P. Protti, AMEL Electrochemistry. Introduction to Modern Voltammetric and Polarographic  
Analysis Techniques (2001), IV Edition.